Checkpoint kinase 2 regulates prostate cancer cell growth through physical interactions with the androgen receptor

Huy Q Ta[1,#], Natalia Dworak[1,#], Melissa L Ivey[1], Devin G. Roller[1], and Daniel Gioeli[1,2,*]

1 Department of Microbiology, Immunology, and Cancer Biology, University of Virginia, Charlottesville, Virginia, United States of America

2 Cancer Center Member, University of Virginia, Charlottesville, Virginia, United States of America

Running title: CHK2 and AR interact to regulate PCa

[#] These authors contributed equally to the work.

***** To whom correspondence should be addressed. Daniel Gioeli, Department of Microbiology, Immunology, and Cancer Biology, University of Virginia, Charlottesville, Virginia, 22908, United States of America; Tel: (1) 434-982-4243; Fax: (1) 434-982-0689; Email: dgioeli@virginia.edu

ABSTRACT

We have previously demonstrated that checkpoint kinase 2 (CHK2) is a critical negative regulator of androgen receptor (AR) transcriptional activity, prostate cancer (PCa) cell growth, and androgen sensitivity. We have now uncovered that the AR directly interacts with CHK2, and ionizing radiation (IR) increases this interaction. This IR-induced increase in AR–CHK2 interactions requires AR phosphorylation and CHK2 kinase activity. PCa associated CHK2 mutants with impaired kinase activity reduced IR-induced AR–CHK2 interactions. The destabilization of AR–CHK2 interactions induced by CHK2 variants impairs CHK2 negative regulation of cell growth. CHK2 depletion increases transcription of DNAPK and RAD54, increases clonogenic survival, and increases resolution of DNA double strand breaks. The data support a model where CHK2 sequesters the AR through direct binding decreasing AR transcription and suppression of PCa cell growth. CHK2 mutation or loss of expression thereby leads to increased AR transcriptional activity and survival in response to DNA damage.

34 **INTRODUCTION**

35 Mammalian cells are continuously being bombarded by endogenous and
36 exogenous forces that jeopardize the integrity of DNA. In response to DNA damage, a
37 conserved network of signaling pathways known as the DNA damage response (DDR) is
38 activated to maintain cell viability and genome stability [1]. Prostate cancer (PCa) remains
39 one of the leading causes of death among men of all races (cdc.gov), as castration-
40 resistant prostate cancer (CRPC) is currently incurable. Recently, the DDR has been a
41 focus of PCa research since the androgen receptor (AR), a major driver of PCa,
42 modulates the transcription of DDR genes and DNA repair [2]–[4]. We have previously
43 shown that checkpoint kinase 2 (CHK2) negatively regulates androgen sensitivity and
44 PCa cell growth [5].

45 CHK2 is a serine/threonine protein kinase that plays a crucial role in sensing DNA
46 damage and initiating the DDR, which is comprised of cell cycle arrest, DNA repair, and
47 apoptosis [6]. CHK2 consists of an amino-terminal SQ/TQ cluster domain (SCD) where
48 threonine 68 serves as a substrate for phosphorylation by ataxia-telangectasia mutated
49 (ATM) kinase [7]; a carboxy-terminal kinase domain (KD) and nuclear localization
50 sequence [8]; and a central forkhead-associated domain (FHA) that provides an interface
51 for interactions with phosphorylated proteins [9]. Currently, there are approximately 24
52 CHK2 substrates in human cells that have been experimentally validated, including polo-
53 like kinase 1 (PLK1), promyelocytic leukemia protein (PML), E2F1, p53, and cell division
54 cycle 25C (CDC25C) [10]. These studies show that one mechanism CHK2 utilizes to
55 affect cellular function is through direct protein-protein interactions.

56 CHK2 association with PLK1 leads to its localization at centrosomes where it
57 regulates mitotic entry [11]. CHK2 autophosphorylation and activation are regulated by
58 the tumor suppressor PML within nuclear matrix-associated structures called PML-
59 nuclear bodies, which are nuclear matrix-associated structures [12]. Binding to PML
60 keeps CHK2 in an inactive state within these PML-nuclear bodies. In return, activated
61 CHK2 can phosphorylate PML on S117 and induce PML-mediated apoptosis. CHK2 can
62 also modify the transcription of apoptotic genes through direct binding and S364
63 phosphorylation of the E2F1 transcription factor in response to DNA damage, thereby
64 stabilizing E2F1 and activating gene transcription [13]. CHK2 also regulates apoptosis
65 through p53 phosphorylation, and promotion of p53-mediated cell death [14]. The
66 interaction with the core domain of p53 induces an allosteric change in CHK2 which
67 permits p53 S20 phosphorylation [15]. Moreover, CHK2 modulates CDC25C localization
68 by associating with and phosphorylating CDC25 on S216, which creates a binding site
69 for 14-3-3 proteins [16]. 14-3-3 proteins in turn sequester CDC25C in the cytoplasm and
70 block the G2/M transition since cyclin dependent kinase 1 (CDK1) cannot be activated.
71 Finally, our group has shown that CHK2 co-immunoprecipitated with AR in PCa cells and
72 regulated growth, suggesting that AR may be a novel substrate of CHK2 [5]. Thus, given
73 the importance of CHK2 and AR to the DDR and prostate cancer growth, a full
74 understanding of the functional consequences of the CHK2–AR interaction is required,
75 with the hope of possible clinical applications towards CRPC.

76 Here, we uncovered novel molecular interactions between CHK2 and AR that
77 provide mechanistic insight into our observation that CHK2 negatively regulates prostate
78 cancer growth. We demonstrate that AR directly binds CHK2, and that this interaction

79 increases with ionizing radiation (IR). The IR-induced increase in AR – CHK2 interaction
80 requires AR phosphorylation on both S81 and S308 and CHK2 kinase activity, which is
81 impaired in PCa associated CHK2 mutations. Furthermore, these CHK2 mutants exhibit
82 diminished effects on prostate cancer cell growth. CHK2 depletion increases transcription
83 of DNAPK and RAD54, clonogenic survival, and resolution of DNA double strand breaks
84 (DSBs) following IR, while altering the kinetics of IR-induced γH2AX foci.
85

86 **RESULTS**

87 **AR directly binds CHK2**

88 We previously showed that AR co-immunoprecipitated with CHK2 immune
89 complexes in several prostate cancer cell lines [5]. To determine whether this co-
90 association was through direct protein-protein interaction, we performed Far Western
91 blotting (Figure 1, Supplemental Figure 1) [17], [18]. We also used Far Western blotting
92 to test the impact of AR phosphorylation on CHK2 binding to AR. We focused on S81 and
93 S308 phosphorylation since the phosphorylation of AR on S81 by CDK1 and CDK9
94 stimulates AR transcriptional activity and growth of PCa cells [19]–[21]. AR
95 phosphorylation on S308 by CDK1 represses AR transcriptional activity and alters AR
96 localization during mitosis [22], [23]. To generate purified protein for the far westerns,
97 293T cells were transfected with mammalian plasmids expressing FLAG-wtAR, or the
98 FLAG-AR mutants S81A, S81D, S308A, or S308D, FLAG-ERK2, or V5-wtCHK2 (Fig. 1A).
99 We used FLAG-ERK2 as a positive control since it has been reported that CHK2
100 physically associates with ERK1/2 in cancer cells [24]. FLAG-ERK and FLAG-AR targets
101 were immunoaffinity purified and resolved by SDS-PAGE. The target proteins (AR wt and
102 phospho-mutants and ERK) on the membrane were probed with purified V5-wtCHK2
103 protein, crosslinked, and stained with V5 antibodies to detect bound V5-wtCHK2.
104 Membranes were also immunoblotted with AR and ERK1/2 antibodies to confirm that the
105 molecular weight of AR and ERK1/2 corresponded with the CHK2 signal, which then
106 indicates direct protein-protein interaction. We found that V5-wtCHK2 bound to FLAG-
107 wtAR, as well as the control FLAG-ERK2 (Figure 1A). Only AR S308A showed a

108 statistically significant reduction in binding to CHK2 (adjusted p=0.035), although all AR
109 phosphorylation mutants trended to decrease association with CHK2.

110 We observed the reciprocal binding of AR and CHK2 by Far Western. Expression,
111 purification, and Far Western blotting were performed as described above using FLAG-
112 wtCHK2 and FLAG-CHK2 mutants K373E or T387N as targets and HA-wtAR as a probe.
113 This also showed that AR and CHK2 directly bind (Figure 1B). In these experiments we
114 also determined whether the CHK2 mutants in PCa with reduced kinase activity bind to
115 AR. The K373E CHK2 mutation impairs CHK2 function suppressing cell growth and
116 promoting survival in response to IR, as a result of reduced kinase activity due to the
117 disruption of CHK2 autophosphorylation [25]. Less is known about the heterozygous
118 missense mutation T387N, but it is reported to diminish kinase activity [26]. We observed
119 reduced AR – CHK2 binding (adj p=0.026) with the CHK2 K373E mutant. No significant
120 change was observed with the CHK2 T387N mutant. These data suggest that the AR
121 directly binds CHK2 and that AR phosphorylation and CHK2 kinase activity may impact
122 that binding.

123 **Radiation increases CHK2-AR association**

124 Since IR is a standard of care for patients with localized advanced PCa, and CHK2
125 is a mediator of the DDR, we wanted to assess the impact of IR on CHK2-AR interactions.
126 Moreover, we wanted to test the influence of AR phosphorylation and CHK2 mutation on
127 any effect of IR on the AR – CHK2 interaction. LNCaP cells were transduced with lentiviral
128 particles containing wtAR or AR mutants S81A or S308A (Fig. 2A). The association of AR
129 was analyzed from endogenous CHK2 immune complexes generated one hour after
130 irradiation. There was a 4-fold increase in AR co-immunoprecipitating with CHK2 after IR

131 treatment of cells expressing wtAR. However, neither S81A nor S308A increased in
132 association with CHK2 upon IR treatment indicating that phosphorylation of AR on S81
133 and S308 are required for the IR-induced increase in the interaction between CHK2 and
134 AR. Interestingly, in contrast to the AR – CHK2 association by Far Western, the basal
135 level of CHK2 and AR co-immunoprecipitation (co-IP) was unaffected by AR
136 phosphorylation.

137 The requirement for AR phosphorylation for the IR-induced increase in AR – CHK2
138 association led us to test if AR phosphorylation on S81 and S308 was increased in
139 response to IR. AR was immunoprecipitated from irradiated cells, and phospho-S81 and
140 phospho-S308 were measured by western blotting using phospho-specific antibodies to
141 those sites [20], [27] (Supplemental Figure 2). There were no significant changes in S81
142 or S308 phosphorylation in response to IR in either cell line. Thus, these findings indicate
143 that while the intensity of S81 and S308 phosphorylation does not markedly change with
144 IR, S81 and S308 phosphorylation is necessary for AR – CHK2 interactions under certain
145 conditions.

146 **CHK2 kinase activity is required for AR – CHK2 interaction**

147 To further determine if CHK2 kinase activity was necessary for the AR – CHK2
148 association and what impact IR has on CHK2 mutant association with AR, we tested if
149 CHK2 mutants that are found in PCa and have impaired kinase activity could interact with
150 the AR by co-IP. We expressed FLAG-wtCHK2, FLAG-K373E, or FLAG-T387N in
151 combination with HA-wtAR in LNCaP cells. FLAG-CHK2 immunoprecipitations were
152 performed and HA-AR association was evaluated (Fig. 2B). In response to IR there was
153 a striking increase in CHK2–AR co-association in cells expressing FLAG-wtCHK2 and

154 HA-wtAR. However, the amount of IR-induced increase in the AR – CHK2 association in
155 cells expressing either K373E or T387N was dramatically reduced. No change in basal
156 AR – CHK2 co-IP was observed. Immunoblotting of cell lysates used in the co-IPs indicate
157 that the differences in co-IPed protiens was not due to protein expression (Figure 2C.
158 These data indicate that the kinase activity of CHK2 is required for the optimal induction
159 of the CHK2 and AR interaction in response to IR, and that the CHK2 mutants associated
160 with PCa have a diminished ability to interact with the AR in irradiated cells.

161 **PCa associated CHK2 mutants limit suppression of PCa growth**

162 Since CHK2 regulates the cell cycle and PCa cell growth [5], [15], we investigated
163 the effect of CHK2 mutations found in PCa, which disrupt the AR – CHK2 interaction, on
164 CHK2 regulation of PCa cell growth (Fig. 3). PCa cells were transduced with vector or
165 shRNA specific to CHK2 to deplete endogenous CHK2, and then CHK2 expression was
166 rescued with wtCHK2, K373E, or T387N. Cell growth was quantitated in the presence
167 and absence of 0.05nM R1881 (synthetic androgen) seven days following transduction
168 using CyQUANT to assess cell proliferation as a function of DNA content. In agreement
169 with previous reports [5], hormone stimulated growth of vector-expressing cells and
170 knockdown of CHK2 significantly augmented growth in all PCa cell lines tested (Fig. 3).
171 Here growth induced by CHK2 knockdown is likely an increase in cell proliferation, as the
172 basal apoptotic rate in the PCa lines is low. Re-expression of wtCHK2, K373E, and T387N
173 in CHK2-depleted cells markedly suppressed the increase in growth induced by CHK2
174 knockdown in all PCa cell lines tested. Interestingly, in LNCaP cells the extent of growth
175 inhibition induced by K373E and T387N was significantly less than that generated by
176 wtCHK2 (Fig. 3A). The effect of CHK2 re-expression on cell growth in castration-resistant

177 C4-2 (Fig. 3B) and Rv1 (Fig. 3C) cells was not significantly different between wtCHK2
178 and the kinase deficient K373E and T387N mutants, although the magnitude of inhibition
179 caused by the mutants was consistently less than that produced by wtCHK2. Expression
180 levels of wtCHK2, K373E, and T387N do not account for the difference observed between
181 LNCaP and C4-2 or Rv1 (Fig. 3) since the relative expression of wtCHK2, K373E, and
182 T387N were similar across the cell lines. These observations suggest that CHK2 kinase
183 activity limits the ability of CHK2 to negatively regulate PCa cell growth, especially in
184 androgen dependent PCa.

185 **CHK2 suppresses IR induction of DNAPK and RAD54**

186 Reports in the literature suggest that the AR is a critical regulator of genes in the
187 DDR [2]–[4] Therefore we evaluated the impact of CHK2 knockdown on IR induced
188 transcription of DDR genes in LNCaP cells (Fig. 4). In our experiments, androgen or IR
189 only modestly affected DNAPK and RAD54 transcript levels; we did not observe androgen
190 or IR induction of XRCC2, XRCC3, XRCC4, XRCC5, MRE11, RAD51, FANC1 and
191 BRCA1 transcripts as reported by others (data not shown) [2], [3]. This discrepancy is
192 consistent with the observation that androgen regulation of DDR genes is specific to the
193 model system, experimental conditions, and disease state examined [4]. Knockdown of
194 CHK2 in LNCaP cells grown in CSS and stimulated with 1nM DHT led to an increase in
195 transcription of DNAPK and RAD54 in response to IR, suggesting that CHK2 may
196 suppress AR transcription of DDR genes in response to IR.

197 **CHK2 effect on IR sensitivity and DNA repair**

198 We next examined the impact of CHK2 interactions on cell survival and sensitivity
199 to IR (Fig. 5A). LNCaP cells expressing CHK2 (pLKO) or depleted of CHK2 (CHK2 KD)

200 were exposed to increasing doses of IR, plated, and allowed to grow for 14 days.
201 Clonogenic assays revealed that CHK2 knockdown promoted cell survival following
202 ionizing radiation. This data, along with the data above indicating that CHK2 suppresses
203 AR transcription of DNA repair genes suggested the hypothesis that loss of CHK2 could
204 facilitate DNA repair.

205 To assess the effect of IR-induced DNA damage in the presence or absence of
206 CHK2 knockdown we performed comet assays to measure DNA breaks [28], and
207 immunofluorescence staining of γH2AX, a marker for DNA double-strand breaks [29],
208 [30]. When we examined DNA damage using the comet assay, we observed statistically
209 significant less DNA breaks with CHK2 knockdown at 24hrs in LNCaP cells (Figure 5B).
210 The comet assay shows less % DNA in tail, shorter DNA tail length, and lower tail moment
211 with CHK2 knockdown suggesting more efficient DNA repair when CHK2 is
212 compromised. In order to quantify DSB repair activity in an unbiased manner, we
213 developed an approach that utilizes automated quantitation of γH2AX and 53BP1 foci
214 detected with immunofluorescence that enables us to rapidly determine the signal
215 intensity (Supplemental Fig. 3). Rv1 cells were transduced with vector or CHK2 shRNA
216 48hrs before IR. Radiation induced more γH2AX foci at 15min when CHK2 was knocked
217 down (Fig.6A, B). However, less foci are found in CHK2 knock-down cells at 2hrs and by
218 4hrs through 24hrs an equal number of foci are present in control and CHK2 knock-down
219 cells. H2AX is phosphorylated in response to inputs in addition to IR induced DNA double
220 strand breaks, including RNA polymerase II dependent transcription [31]–[33]. Therefore,
221 we also measured 53BP1 foci to assess DSB repair and found no significant differences
222 when CHK2 was knocked down (Fig 6C). The apparent discrepancy in the 53BP1 and

223 γH2AX foci may be explained by an increase in transcription when CHK2 is knocked
224 down, as shown in Figure 4 and in our previous study [5].
225 Since superphysiological doses of androgen has been associated with
226 transcription dependent double strand breaks [34], [35], we also tested if CHK2
227 knockdown would augment superphysiological androgen dependent γH2AX foci. LNCaP
228 and Rv1 cells were transduced with vector or CHK2 shRNA 48 hours before treatment
229 with a range of the synthetic androgen R1881 up to 100nM for 6 hours (Supplemental
230 Fig. 4). We saw modest hormone induced γH2AX foci and no change with CHK2
231 knockdown. The superphysiologic dose of androgen likely maximally activates AR
232 dependent transcription negating the increase in AR transcriptional activity typically
233 observed with CHK2 knockdown.
234

235 **DISCUSSION**

236 PCa is the most frequently diagnosed cancer and the second leading cause of
237 cancer death among American men, with approximately 88 men dying from PCa every
238 day (pcf.org). While androgen deprivation therapy (ADT) is effective initially, most patients
239 will relapse and develop incurable CRPC. Recently, there has been an emphasis on
240 understanding the link between the DDR and AR, since radiation is a standard of care for
241 locally advanced PCa where the AR is a major driver, and PARP inhibitors may be
242 efficacious in CRPC patients with mutations in DDR genes [2], [3], [5], [36]–[38].

243 Our study identifies AR as a direct interacting protein with CHK2 in PCa cells.
244 Several studies elucidated the role of DDR protein-AR interactions in modulating AR
245 transcriptional activity. PARP-1 was recruited to AR binding sites, enhancing AR
246 occupancy and transcriptional function [39]. Tandem mass spectroscopy analysis
247 identified Ku70 and Ku80 as direct AR-interacting proteins that positively regulate AR
248 transactivation [40]. Furthermore, BRCA1 physically interacted with the DNA-binding
249 domain (DBD) of AR to enhance AR transactivation and induce androgen-mediated cell
250 death through p21 expression [41]. In contrast, the association of the LBD of AR with
251 hRad9, a crucial member of the checkpoint Rad family, suppressed AR transactivation by
252 preventing the androgen-induced interaction between the n-terminus and c-terminus of
253 AR [42]. Other groups reported non-genomic effects as a result of DDR protein-AR
254 interactions. Mediator of DNA damage checkpoint protein 1 (MDC1), an essential player
255 in the Intra-S phase and G2/M checkpoints, physically associated with FL-AR and AR^{V7}
256 to negatively regulate PCa cell growth and migration [43]. Yin and colleagues, on the
257 other hand, showed that increased clonogenic survival following IR was a consequence

258 of DNA-PKc directly complexing with both FL-AR and AR^{V5-7}, with radiation increasing
259 these interactions and enzalutamide blocking the association with FL-AR but not AR^{V5-7}
260 [44]. These data support a model where AR is integrated in the DDR, interfacing at
261 multiple points.

262 We show that the direct association of CHK2 and AR by Far Western requires
263 phosphorylation of AR on S308. Since proteins containing FHA domains bind
264 phosphoproteins [9], we hypothesize that AR interacts with CHK2 through the CHK2 FHA
265 domain. In support of this, the Zhao lab determined that AR physically associated with
266 the FHA domain of another critical DDR member, MDC1 [43]. Expression of truncation
267 mutants of different MDC1 domains in LNCaP cells led to the discovery that AR only co-
268 immunoprecipitated with MDC1 mutants containing the FHA domain in the absence and
269 presence of dihydrotestosterone. Their results indicated that the FHA domain of MDC1
270 mediated the interaction with AR.

271 Here we report that AR phosphorylation on S81 and S308 is required for the IR
272 induction of AR – CHK2 binding by co-IP. Interestingly neither of these phosphorylation
273 sites were altered by IR. AR S81 and S308 can both be phosphorylated by CDK1, which
274 is downstream of canonical CHK2 signaling [21], [27], and was the motivation for
275 examining these sites in response to IR. The prediction is that IR would lead to a decrease
276 in S81 and S308 phosphorylation. However, our previous studies demonstrated that S81
277 is predominantly phosphorylated by CDK9, and thus is more indicative of AR
278 transcriptional activity [20]. We also found that S308 phosphorylation was restricted to
279 late G2 and M phase of the cell cycle [27]. CDK9 phosphorylation of S81 and the
280 restriction of S308 phosphorylation to G2/M likely accounts for the lack of significant

281 change in these phosphorylation sites in response to IR. The disconnect between these
282 sites being required for the IR induced increase in AR – CHK2 association but not being
283 regulated by IR suggests that the hormone induced activation state of the AR is a critical
284 determinant in the IR induced increase in AR – CHK2 association. We observed
285 differences when testing the AR – CHK2 association by Far Western and co-IP. The direct
286 protein-protein interaction is only impacted by loss of S308 phosphorylation, however,
287 basal co-IP of AR and CHK2 is not affected by AR phosphorylation. Only the IR induced
288 AR – CHK2 association is impacted by loss of AR phosphorylation on S81 and S308. This
289 suggests that additional proteins present in cells may assist and participate in the AR –
290 CHK2 interaction.

291 We found that CHK2 variants with diminished kinase activity impaired the IR-
292 induced increase in AR – CHK2 interaction but did not completely block the interaction.
293 As with AR phosphorylation, there were differences when the CHK2 mutant association
294 with AR was examined by Far Western or co-IP suggesting a more complicated dynamic
295 of AR – CHK2 association in cells. The PCa associated CHK2 mutants also exhibited a
296 reduced inhibition of cell growth. CHK2-depleted cells re-expressing CHK2 variants
297 exhibited an approximate 2-3-fold reduction in growth inhibition in response to hormone
298 when compared to cells re-expressing wtCHK2. Moreover, the fold change in growth
299 suppression between wtCHK2 and CHK2 variants was greater in androgen-dependent
300 LNCaP cells than in castration-resistant C4-2 and Rv1 cells, suggesting that in hormone
301 sensitive PCa CHK2 variants may play a larger role in regulating growth. This raises the
302 possibility that the CHK2 mutants found in PCa with diminished AR binding are selected
303 for, decreasing CHK2 suppression of AR activity and PCa cell growth. Berge and

304 colleagues discovered numerous CHK2 splice variants in breast cancer tissue, where all
305 variants were co-expressed with wtCHK2 [45]. Furthermore, several of these variants
306 reduced kinase activity when simultaneously expressed with wtCHK2 and displayed a
307 dominant negative effect on wtCHK2. The impact of the CHK2 variants found in PCa on
308 wtCHK2 function has not yet been fully explored.

309 In our experiments examining AR – CHK2 binding, ERK was used as a positive
310 control for a protein that interacts with CHK2 [24]. Interestingly, we observed a significant
311 increase in CHK2–ERK association with IR. This is consistent with IR increasing CHK2
312 T68 phosphorylation, which is required for the CHK2–ERK interaction. These data point
313 to a potentially larger role for CHK2 beyond canonical DDR and cell cycle checkpoint
314 signaling; consistent with this notion CHK2 has been implicated in diverse cellular
315 processes [46]–[48]. MEK inhibition is effective in lung tumors with ATM mutations where
316 CHK2 is inactive [49] providing further support that CHK2 negatively regulates ERK.
317 Negative regulation of both the AR and ERK by CHK2 suggests the hypothesis that CHK2
318 may serve as a general negative regulator of mitogenic signals in response to IR.

319 Multiple studies indicate that the AR is a critical regulator of genes in the DDR [2],
320 [3]. Reports by others demonstrate that androgen and IR increased DNAPK, XRCC2, and
321 XRCC3 [3]. This concept was supported by more global analysis of transcripts
322 demonstrating androgen regulation of DDR genes [2]. Another global analysis identified
323 a different set of DDR genes are regulated by AR [4]. Our test by RT-qPCR of ten different
324 DDR genes found only a modest induction by IR or androgen treatment in two DDR
325 genes, DNAPK and RAD54. The discrepancy in the DDR gene subsets regulated by the
326 AR in these studies and ours may be system dependent. However, it also indicates that

327 the dogma of AR regulating DDR genes needs further examination. Our data indicating
328 that CHK2 knockdown increases DNAPK and RAD54 transcript levels is consistent with
329 our earlier observation that CHK2 knockdown led to the increase in the transcripts of
330 canonical AR target genes [5]. This leads to the hypothesis that CHK2 binding to the AR
331 suppresses AR transcription of DDR genes enabling cells to turn off the DDR following
332 DNA repair.

333 We observed radiation resistance in CHK2 knockdown cells. We also observed an
334 increase in γH2AX signal when CHK2 was knocked down, and a decrease in DNA breaks
335 as measured by the comet assay under similar conditions. However, when 53BP1 signal
336 was measured to assess DSB repair we found no significant differences when CHK2 was
337 knocked down. These conflicting results of γH2AX and 53BP1 signal may be explained
338 by phosphorylation of H2AX in response to transcription induced DNA breaks [31]–[33].
339 These incongruous results may also be due to competing effects of CHK2 as both a
340 regulator of the cell cycle and apoptosis [46].

341 The data reported herein along with our previous work [5] indicate that CHK2 acts
342 as a tumor suppressor in PCa, either through loss of expression or mutation. This raises
343 the concern that CHK2 antagonists in clinical development may paradoxically lead to
344 enhanced PCa growth and resistance to IR. However, it is important to note that we have
345 predominately used an RNAi/overexpression approach. Our RNAi approach is more
346 similar to the CHK2 variants in PCa that have reduced kinase activity. It is important to
347 consider that pharmacologic inhibition is different than inhibition by RNAi [50]. A
348 pharmacologic approach that provides a sudden and complete inhibition of CHK2 kinase
349 activity may impact PCa differently than our RNAi approach, especially when combined

350 with IR or AR antagonists. However, our work and that in the literature also suggests that
351 approaches downstream of CHK2 may be more straightforward than targeting CHK2.
352 In this study, we presented data that provides mechanistic insight into our
353 observation that CHK2 negatively regulates PCa growth. We demonstrated that AR
354 directly bound CHK2, and that IR elevated the AR – CHK2 interaction. Not only did these
355 AR – CHK2 protein complexes require AR phosphorylation, but CHK2 kinase activity was
356 also necessary. Furthermore, these CHK2 mutants found in PCa exhibited a diminished
357 effect on restricting prostate cancer cell growth. We observed that knockdown of CHK2
358 led to an increase in PCa cell survival and resolution of DNA DSBs in response to IR.
359 This suggests that the deregulation of CHK2 in PCa can confer resistance to radiation. In
360 a previous study, we showed that CHK2 knockdown hypersensitized PCa cells to castrate
361 levels of androgen and increased AR transcriptional activity on both androgen-activated
362 and androgen-repressed genes [5]. As part of a feedback loop, AR transcriptionally
363 represses CHK2 levels. Thus, these data along with our previously published results
364 suggest the following model (Figure 7). Wild-type CHK2 maintains homeostasis through
365 mediating the balance between DNA repair and cell death, antagonizes the AR through
366 direct binding and inhibition of transcription of AR target genes while AR transcriptionally
367 represses CHK2. This feedback loop enables AR repression of CHK2 to turn off the DDR,
368 while CHK2 negatively regulates AR to dampen growth during repair of damaged DNA.
369 CHK2 mutation or loss of expression in PCa leads to increased AR transcriptional activity,
370 possibly of DDR genes, and survival in response to DNA damage, all leading to a more
371 aggressive cancer. Collectively, the work provides a foundation for the continued study
372 of AR – CHK2 interactions and functional consequences to benefit PCa therapies.

374 **MATERIALS AND METHODS**

375 **Cell culture**

376 LNCaP and C4-2 cells (a gift from Dr. L. W. K. Chung) were grown in DMEM:F12
377 (Invitrogen) with 5% non-heat inactivated serum (Gemini) and 1% Insulin-Transferrin-
378 Selenium-Ethanolamine (ITS) (ThermoFisher). CWR22Rv1 (Rv1) (gift from Drs. Steven
379 Balk) and 293T cells (gift from Dr. Tim Bender) were grown in DMEM (Invitrogen) with
380 10% heat-inactivated serum. For growth experiments, phenol-red free DMEM:F12 media
381 with 5% Charcoal-Stripped Serum (CSS) (Sigma) was used. Commercial DNA
382 fingerprinting kits (DDC Medical) verified cell lines. The following STR markers were
383 tested: CSF1PO, TPOX, TH01, Amelogenin, vWA, D16S539, D7S820, D13S317 and
384 D5S818. Allelic score data revealed a pattern related to the scores reported by the ATCC,
385 and consistent with their presumptive identity.

386 **Reagents**

387 Transfection: Fugene 6 (Promega); TransIT-2020 (Mirus Bio). Inhibitors:
388 Enzalutamide (Selleck Chemicals), BML-277 (Santa Cruz Biotech). Antibodies: CHK2
389 (2G1D5), pCHK2 T68, ERK1/2 (137F5), Actin, Flag-Tag, V5-Tag, HA-Tag, γH2AX (Cell
390 Signaling); AR, pAR S308 (in-house); pAR S81 (Millipore); Cy3-labeled donkey anti-rabbit
391 (Jackson ImmunoResearch). Western blotting performed as previously described [5].

392 **Far Western Blot**

393 To measure direct protein interactions, the protocol was adapted from Prickett *et*
394 *al* [17] and Wu *et al* [18]. 293T cells were transfected with FLAG-wtAR, FLAG-S81A,
395 S81D, S308A, S308D, HA-wtAR, FLAG-ERK2, V5-wtCHK2, FLAG-CHK2, FLAG-CHK2
396 mutants K373E or T387N, or empty vector control. Whole cell extracts were made using

397 Triton-X lysis buffer, sonicated, and immunopurified using anti-FLAG, anti-HA, or anti-V5
398 beads (Sigma) for 2hr at 4°C. Protein bound to beads was washed three times with Triton-
399 X lysis buffer, eluted with 35μl 2X sample buffer, and boiled for 5 min. Proteins were
400 resolved by SDS-PAGE and transferred to PVDF membrane. Proteins on the membrane
401 were denatured and renatured in buffers with varying guanidine–HCl concentrations.
402 Membranes were blocked in 3% blocking buffer (3% bovine serum albumin in Tris-
403 buffered saline/Tween 20) for 1hr. Probes were diluted in 3% blocking buffer and
404 incubated overnight at 4°C. Membranes were washed three times with PBS for 5min
405 followed by fixation using 0.5% paraformaldehyde for 30 min at room temperature.
406 Membranes were then rinsed quickly twice with PBS and quenched using 2% glycine in
407 PBS for 10 min at room temperature. The membrane was blotted for FLAG, HA, V5, AR,
408 CHK2, or ERK1/2 and analyzed using the LI-COR Odyssey system and software.

409 **Immunoprecipitation**

410 CHK2 or AR protein was immunoprecipitated from 1mg cell lysate from LNCaP
411 cells transiently transfected with FLAG-wtAR/FLAG-S81A/FLAG-S308A or FLAG-
412 wtCHK2/Flag-K373E/Flag-T387N plus HA-wtAR for 48hrs; treated with radiation.
413 Immunoprecipitations were performed with either agarose or magnetic beads, proteins
414 were separated by 7.5% SDS-PAGE; and immunoblotted with AR, pAR S81, pAR S308,
415 CHK2, pCHK2 T68, HA, or ERK1/2 antibodies.

416 **CyQuant Growth Assays**

417 Assay was performed as previously described [5]. Briefly, shCHK2-209, shCHK2-
418 588, wtCHK2, K373E, T387N or Vector control virus was added to fibronectin-coated
419 (1μg/ml) 96well plates. Constructs of CHK2 wild-type and variants were verified by

420 sequencing. Cells were plated in phenol-red free DMEM:F12 or DMEM media with 5%
421 CSS in the presence or absence of 0.05nM R1881. CyQuant reagent was added on day
422 7 according to the manufacturer's protocol (ThermoFisher). Quantification was performed
423 using a BioTek Synergy 2 plate reader.

424 **qPCR**

425 RNA isolation and quantitative real-time PCR (qPCR) were performed as
426 previously described [51], [52]. RNA concentrations were determined using a NanoDrop
427 2000 UV-Vis Spectrophotometer (Thermo Scientific). Primer sequences and annealing
428 temperature: DNAPKc FW (ATGAGTACAAGCCCTGAG); DNAPKc RV
429 (ATATCAGAGCGTGAGAGC) (Tm=60deg). RAD54B FW
430 (ATAACAGAGATAATTGCAGTGG); RAD54B RV (GATCTAATGTTGCCAGTGTAG)
431 (Tm=60deg). PSMB6 FW (CAAACTGCACGGCCATGATA); PSMB6 RV
432 (GAGGCATTCACTCCAGACTGG) (Tm=60deg).

433 **Clonogenic Survival Assay**

434 LNCaP cells were transduced with lentiviral particles expressing vector or CHK2
435 shRNAs and treated with 0-6Gy of radiation 72hrs after transduction. Cells were
436 trypsinized, counted, and appropriate numbers were plated in triplicate with the
437 appropriate growth media for colony formation assays (100 cells/0Gy, 200 cells/2Gy,
438 1000 cells/4Gy, and 6000 cells/6Gy). After 10-14 days, colonies consisting of 50-70 cells
439 were counted using crystal violet. Plotted is the surviving fraction (number of colonies
440 counted/(number of cells seeded x PE) where PE = plating efficiency = number of colonies
441 counted/number of cells seeded) following radiation.

442 **Comet Assay**

443 All Comet Assay steps were performed in the dark. Cells were washed twice with
444 PBS, scraped and suspended in PBS. Cells were combined with molten LMAgarose
445 (Trevigen, 4250-050-02) and placed into comet suitable slides. Samples were left at 4°C
446 for 15 minutes in order to create a flat surface. Slides were immersed in lysis solution
447 (Trevigen, 4250-050-01) for 40 minutes at 4°C and then in alkaline solution for 30min at
448 room temperature. Slides were electrophoresed in 200mM NaOH, 1mM EDTA in water;
449 pH>13 at 21Volts (300mA) for 30 minutes at 4°C. After the electrophoresis, slides were
450 gently drained, washed twice in dH2O for 10min and immersed in 70% ethanol for 5min.
451 Samples were left to dry overnight at RT. Samples were stained with SYBR Green at 4°C
452 for 5 minutes and left to dry completely overnight. For quantification, images were
453 acquired using a fluorescence microscope (Olympus BX51, High-mag) equipped with a
454 20×, 0.5 NA objective and a camera (DP70). Images were acquired with DPController
455 software. Images were analyzed by ImageJ software and graphs generated using Prism
456 (GraphPad Software). All imaging was performed at ~24°C.

457 **Immunofluorescence (IF)**

458 LNCaP cells were transduced with lentivirus expressing vector or CHK2 shRNAs
459 on 1μg/ml fibronectin-coated coverslips and treated with radiation 48hrs after
460 transduction. Cells were allowed to recover from IR exposure up to 24hrs. Coverslips
461 were washed 3X with PBS, permeabilized with 0.2% Triton-X for 5mins, washed 3x quick
462 and 3x 5min with PBS-Tween 20 at 0.05% (PBS-T), blocked with 2% FBS/BSA/donkey
463 serum in PBS-T for 2hrs at room temperature, and incubated with γH2AX or 53BP1
464 antibodies overnight at 4°C. Coverslips were then washed by rocking for 3x quick and 3x
465 10min in PBS-T and incubated with donkey anti-rabbit or anti-mouse secondary antibody

466 (Invitrogen) for 1hr at room temperature. Coverslips were then washed by rocking for 3x
467 quick and 3x 10min in PBS-T and mounted with Vectashield containing DAPI
468 (ThermoFisher). Images were acquired with a LSM 880 confocal microscope (Carl Zeiss)
469 and signals were measured using ImageJ software.

470 **Scientific Rigor**

471 Each experiment was performed independently a minimum of three times and
472 each experiment had technical replicates for measuring the endpoint. An independent
473 experiment is defined as an experiment performed on a different day with a different cell
474 line passage number. The number of independent experiments is reported in each figure
475 legend. All data are shown, no outliers were removed. Statistical analysis was performed
476 using GraphPad Prism 8.2.1 and the test used is reported in each figure legend.

477

ACKNOWLEDGEMENTS

We thank the members of the laboratories of Drs. Gioeli, Jameson, Bouton, Dudley, Kashatus, Park, Rutkowski, Smith, and Zong for helpful discussions.

FUNDING

This work was supported by the National Cancer Institute [R01 CA178338 to DG]; Paul Mellon Urologic Cancer Institute; and University of Virginia Cancer Center Patient and Friends.

COMPETING INTERESTS

The authors declare no competing financial interests

REFERENCES

[1] N. Rhind and P. Russell, “Chk1 and Cds1: linchpins of the DNA damage and replication checkpoint pathways,” *J. Cell. Sci.*, vol. 113 (Pt 22), pp. 3889–3896, Nov. 2000.

[2] W. R. Polkinghorn *et al.*, “Androgen receptor signaling regulates DNA repair in prostate cancers,” *Cancer Discov*, vol. 3, no. 11, pp. 1245–1253, Nov. 2013, doi: 10.1158/2159-8290.CD-13-0172.

[3] J. F. Goodwin *et al.*, “A hormone-DNA repair circuit governs the response to genotoxic insult,” *Cancer Discov*, vol. 3, no. 11, pp. 1254–1271, Nov. 2013, doi: 10.1158/2159-8290.CD-13-0108.

[4] K. Jividen, K. Z. Kedzierska, C.-S. Yang, K. Szlachta, A. Ratan, and B. M. Paschal, “Genomic analysis of DNA repair genes and androgen signaling in prostate cancer,” *BMC Cancer*, vol. 18, no. 1, p. 960, Oct. 2018, doi: 10.1186/s12885-018-4848-x.

[5] H. Q. Ta *et al.*, “Checkpoint Kinase 2 Negatively Regulates Androgen Sensitivity and Prostate Cancer Cell Growth,” *Cancer Res.*, vol. 75, no. 23, pp. 5093–5105, Dec. 2015, doi: 10.1158/0008-5472.CAN-15-0224.

[6] S. Matsuoka, M. Huang, and S. J. Elledge, “Linkage of ATM to cell cycle regulation by the Chk2 protein kinase,” *Science*, vol. 282, no. 5395, pp. 1893–1897, Dec. 1998.

[7] S. T. Kim, D. S. Lim, C. E. Canman, and M. B. Kastan, “Substrate specificities and identification of putative substrates of ATM kinase family members,” *J. Biol. Chem.*, vol. 274, no. 53, pp. 37538–37543, Dec. 1999.

[8] J. Ahn, M. Urist, and C. Prives, “The Chk2 protein kinase,” *DNA Repair (Amst.)*, vol. 3, no. 8–9, pp. 1039–1047, Sep. 2004, doi: 10.1016/j.dnarep.2004.03.033.

[9] J. Li *et al.*, “Structural and functional versatility of the FHA domain in DNA-damage signaling by the tumor suppressor kinase Chk2,” *Mol. Cell*, vol. 9, no. 5, pp. 1045–1054, May 2002.

[10] C. García-Limones *et al.*, “CHK2 stability is regulated by the E3 ubiquitin ligase SIAH2,” *Oncogene*, vol. 35, no. 33, pp. 4289–4301, 18 2016, doi: 10.1038/onc.2015.495.

[11] L. Tsvetkov, X. Xu, J. Li, and D. F. Stern, “Polo-like kinase 1 and Chk2 interact and co-localize to centrosomes and the midbody,” *J. Biol. Chem.*, vol. 278, no. 10, pp. 8468–8475, Mar. 2003, doi: 10.1074/jbc.M211202200.

[12] S. Yang, C. Kuo, J. E. Bisi, and M. K. Kim, “PML-dependent apoptosis after DNA damage is regulated by the checkpoint kinase hCds1/Chk2,” *Nat. Cell Biol.*, vol. 4, no. 11, pp. 865–870, Nov. 2002, doi: 10.1038/ncb869.

[13] C. Stevens, L. Smith, and N. B. La Thangue, “Chk2 activates E2F-1 in response to DNA damage,” *Nat. Cell Biol.*, vol. 5, no. 5, pp. 401–409, May 2003, doi: 10.1038/ncb974.

[14] A. Hirao *et al.*, “DNA damage-induced activation of p53 by the checkpoint kinase Chk2,” *Science*, vol. 287, no. 5459, pp. 1824–1827, Mar. 2000.

[15] J. Bartek and J. Lukas, “Chk1 and Chk2 kinases in checkpoint control and cancer,” *Cancer Cell*, vol. 3, no. 5, pp. 421–429, May 2003.

535 [16] C. Y. Peng, P. R. Graves, R. S. Thoma, Z. Wu, A. S. Shaw, and H. Piwnica-
536 Worms, “Mitotic and G2 checkpoint control: regulation of 14-3-3 protein binding by
537 phosphorylation of Cdc25C on serine-216,” *Science*, vol. 277, no. 5331, pp. 1501–
538 1505, Sep. 1997.
539 [17] T. D. Prickett *et al.*, “TAB4 stimulates TAK1-TAB1 phosphorylation and binds
540 polyubiquitin to direct signaling to NF-kappaB,” *J. Biol. Chem.*, vol. 283, no. 28, pp.
541 19245–19254, Jul. 2008, doi: 10.1074/jbc.M800943200.
542 [18] Y. Wu, Q. Li, and X.-Z. Chen, “Detecting protein-protein interactions by Far western
543 blotting,” *Nat Protoc*, vol. 2, no. 12, pp. 3278–3284, 2007, doi:
544 10.1038/nprot.2007.459.
545 [19] S. Chen, Y. Xu, X. Yuan, G. J. Bubley, and S. P. Balk, “Androgen receptor
546 phosphorylation and stabilization in prostate cancer by cyclin-dependent kinase 1,”
547 *Proc Natl Acad Sci U S A*, 2006, [Online]. Available:
548 http://www.ncbi.nlm.nih.gov/entrez/query.fcgi?cmd=Retrieve&db=PubMed&dopt=Ci
549 tation&list_uids=17043241.
550 [20] V. Gordon *et al.*, “CDK9 regulates AR promoter selectivity and cell growth through
551 serine 81 phosphorylation,” *Mol Endocrinol*, vol. 24, pp. 2267–80, 2010.
552 [21] S. Chen, S. Gulla, C. Cai, and S. P. Balk, “Androgen receptor serine 81
553 phosphorylation mediates chromatin binding and transcriptional activation,” *J. Biol.*
554 *Chem.*, vol. 287, no. 11, pp. 8571–8583, Mar. 2012, doi:
555 10.1074/jbc.M111.325290.
556 [22] D. Gioeli *et al.*, “Androgen receptor phosphorylation. Regulation and identification
557 of the phosphorylation sites,” *J Biol Chem*, vol. 277, pp. 29304–14, 2002.
558 [23] H. Zong *et al.*, “Cyclin D3/CDK11p58 complex is involved in the repression of
559 androgen receptor,” *Mol Cell Biol*, vol. 27, pp. 7125–42, 2007.
560 [24] B. Dai *et al.*, “Functional and molecular interactions between ERK and CHK2 in
561 diffuse large B-cell lymphoma,” *Nat Commun*, vol. 2, p. 402, 2011, doi:
562 10.1038/ncomms1404.
563 [25] M. Higashiguchi *et al.*, “Clarifying the biological significance of the CHK2 K373E
564 somatic mutation discovered in The Cancer Genome Atlas database,” *FEBS Lett.*,
565 Oct. 2016, doi: 10.1002/1873-3468.12449.
566 [26] M. Wasielewski *et al.*, “Deleterious CHEK2 1100delC and L303X mutants identified
567 among 38 human breast cancer cell lines,” *Breast Cancer Res. Treat.*, vol. 113, no.
568 2, pp. 285–291, Jan. 2009, doi: 10.1007/s10549-008-9942-3.
569 [27] Y. Koryakina, K. E. Knudsen, and D. Gioeli, “Cell-cycle-dependent regulation of
570 androgen receptor function,” *Endocr. Relat. Cancer*, vol. 22, no. 2, pp. 249–264,
571 Apr. 2015, doi: 10.1530/ERC-14-0549.
572 [28] A. R. Collins, “The comet assay for DNA damage and repair: principles,
573 applications, and limitations,” *Mol. Biotechnol.*, vol. 26, no. 3, pp. 249–261, Mar.
574 2004, doi: 10.1385/MB:26:3:249.
575 [29] J. Vignard, G. Mirey, and B. Salles, “Ionizing-radiation induced DNA double-strand
576 breaks: a direct and indirect lighting up,” *Radiother Oncol*, vol. 108, no. 3, pp. 362–
577 369, Sep. 2013, doi: 10.1016/j.radonc.2013.06.013.
578 [30] W. M. Bonner *et al.*, “γH2AX and cancer,” *Nature Reviews Cancer*, vol. 8, no. 12,
579 pp. 957–967, Dec. 2008, doi: 10.1038/nrc2523.

[31] I. Singh *et al.*, “High mobility group protein-mediated transcription requires DNA damage marker γ-H2AX,” *Cell Res.*, vol. 25, no. 7, pp. 837–850, Jul. 2015, doi: 10.1038/cr.2015.67.
[32] H. Bunch *et al.*, “Transcriptional elongation requires DNA break-induced signalling,” *Nature Communications*, vol. 6, p. 10191, Dec. 2015, doi: 10.1038/ncomms10191.
[33] J.-H. Ji *et al.*, “De novo phosphorylation of H2AX by WSTF regulates transcription-coupled homologous recombination repair,” *Nucleic Acids Res.*, vol. 47, no. 12, pp. 6299–6314, Jul. 2019, doi: 10.1093/nar/gkz309.
[34] M. C. Haffner *et al.*, “Androgen-induced TOP2B-mediated double-strand breaks and prostate cancer gene rearrangements,” *Nat. Genet.*, vol. 42, no. 8, pp. 668–675, Aug. 2010, doi: 10.1038/ng.613.
[35] P. Chatterjee *et al.*, “Supraphysiological androgens suppress prostate cancer growth through androgen receptor-mediated DNA damage,” *J. Clin. Invest.*, vol. 130, Jul. 2019, doi: 10.1172/JCI127613.
[36] J. Mateo *et al.*, “DNA-Repair Defects and Olaparib in Metastatic Prostate Cancer,” *N. Engl. J. Med.*, vol. 373, no. 18, pp. 1697–1708, Oct. 2015, doi: 10.1056/NEJMoa1506859.
[37] L. Li *et al.*, “Targeting poly(ADP-ribose) polymerase and the c-Myb-regulated DNA damage response pathway in castration-resistant prostate cancer,” *Sci Signal*, vol. 7, no. 326, p. ra47, May 2014, doi: 10.1126/scisignal.2005070.
[38] Y. Yin *et al.*, “Chk1 inhibition potentiates the therapeutic efficacy of PARP inhibitor BMN673 in gastric cancer,” *Am J Cancer Res*, vol. 7, no. 3, pp. 473–483, 2017.
[39] M. J. Schiewer *et al.*, “Dual roles of PARP-1 promote cancer growth and progression,” *Cancer Discov*, vol. 2, no. 12, pp. 1134–1149, Dec. 2012, doi: 10.1158/2159-8290.CD-12-0120.
[40] G. L. Mayeur, W. J. Kung, A. Martinez, C. Izumiya, D. J. Chen, and H. J. Kung, “Ku is a novel transcriptional recycling coactivator of the androgen receptor in prostate cancer cells,” *J Biol Chem*, vol. 280, pp. 10827–33, 2005.
[41] S. Yeh *et al.*, “Increase of androgen-induced cell death and androgen receptor transactivation by BRCA1 in prostate cancer cells,” *Proc. Natl. Acad. Sci. U.S.A.*, vol. 97, no. 21, pp. 11256–11261, Oct. 2000, doi: 10.1073/pnas.190353897.
[42] L. Wang *et al.*, “Human checkpoint protein hRad9 functions as a negative coregulator to repress androgen receptor transactivation in prostate cancer cells,” *Mol. Cell. Biol.*, vol. 24, no. 5, pp. 2202–2213, Mar. 2004.
[43] C. Wang *et al.*, “MDC1 functionally identified as an androgen receptor co-activator participates in suppression of prostate cancer,” *Nucleic Acids Res.*, vol. 43, no. 10, pp. 4893–4908, May 2015, doi: 10.1093/nar/gkv394.
[44] Y. Yin *et al.*, “Androgen Receptor Variants Mediate DNA Repair after Prostate Cancer Irradiation,” *Cancer Res.*, vol. 77, no. 18, pp. 4745–4754, 15 2017, doi: 10.1158/0008-5472.CAN-17-0164.
[45] E. O. Berge, V. Staalesen, A. H. Straume, J. R. Lillehaug, and P. E. Lønning, “Chk2 splice variants express a dominant-negative effect on the wild-type Chk2 kinase activity,” *Biochim. Biophys. Acta*, vol. 1803, no. 3, pp. 386–395, Mar. 2010, doi: 10.1016/j.bbamcr.2010.01.005.

[46] L. Zannini, D. Delia, and G. Buscemi, “CHK2 kinase in the DNA damage response and beyond,” *J Mol Cell Biol*, vol. 6, no. 6, pp. 442–457, Dec. 2014, doi: 10.1093/jmcb/mju045.

[47] H.-H. Choi *et al.*, “CHK2 kinase promotes pre-mRNA splicing via phosphorylating CDK11(p110),” *Oncogene*, vol. 33, no. 1, pp. 108–115, Jan. 2014, doi: 10.1038/onc.2012.535.

[48] T. Choudhuri, S. C. Verma, K. Lan, M. Murakami, and E. S. Robertson, “The ATM/ATR signaling effector Chk2 is targeted by Epstein-Barr virus nuclear antigen 3C to release the G2/M cell cycle block,” *J. Virol.*, vol. 81, no. 12, pp. 6718–6730, Jun. 2007, doi: 10.1128/JVI.00053-07.

[49] M. Smida *et al.*, “MEK inhibitors block growth of lung tumours with mutations in ataxia-telangiectasia mutated,” *Nat Commun*, vol. 7, p. 13701, 06 2016, doi: 10.1038/ncomms13701.

[50] K. J. Jensen, C. B. Moyer, and K. A. Janes, “Network Architecture Predisposes an Enzyme to Either Pharmacologic or Genetic Targeting,” *Cell Syst*, vol. 2, no. 2, pp. 112–121, Feb. 2016, doi: 10.1016/j.cels.2016.01.012.

[51] V. Gordon *et al.*, “CDK9 regulates AR promoter selectivity and cell growth through serine 81 phosphorylation,” *Molecular Endocrinology (Baltimore, Md.)*, vol. 24, no. 12, pp. 2267–2280, Dec. 2010, doi: 10.1210/me.2010-0238.

[52] H. Whitworth *et al.*, “Identification of Kinases Regulating Prostate Cancer Cell Growth Using an RNAi Phenotypic Screen,” *PLoS ONE*, vol. 7, no. 6, Jun. 2012, doi: 10.1371/journal.pone.0038950.

648 **FIGURE LEGEND**

649 **Figure 1. CHK2 directly binds AR.** 293T cells were transfected with Vector, FLAG-
650 wtAR, or the FLAG-AR mutants S81A, S81D, S308A, or S308D, FLAG-wtCHK2, FLAG-
651 CHK2 mutants K373E or T387N, FLAG-ERK2, HA-wtAR, or V5-wtCHK2 using Fugene
652 6. 48hrs following transfection, FLAG, HA, and V5 were immunoprecipitated, and far
653 western blotting was performed. Membranes were blotted with the following antibodies:
654 FLAG, HA, V5, AR, CHK2, and ERK2. Blots were visualized using the Odyssey CLx. (A)
655 Probe = V5-wild-type CHK2; Targets = FLAG-wtAR, or the FLAG-AR mutants S81A,
656 S81D, S308A, or S308D, and FLAG-ERK2. Representative blots are shown, n=3. (B)
657 Probe = HA-wtAR; Targets = FLAG-wtCHK2, FLAG-CHK2 mutants K373E or T387N.
658 Representative blots are shown, n=4. For (A) and (B), graphs are of relative AR – CHK2
659 binding. Error bars, SEM. Statistical differences were tested for using ANOVA with
660 Dunnett's multiple comparisons test.

661

662 **Figure 2. AR phosphorylation and CHK kinase activity regulates AR – CHK2**
663 **association.** (A) AR – CHK2 interactions requires AR phosphorylation on S81 and S308.
664 LNCaP cells were transduced with lentiviral particles expressing wtAR, S81A, or S308A
665 for 48hrs. Cells were irradiated with 6Gy, and CHK2 was immunoprecipitated one hour
666 after IR. Representative blots are shown. Blots were quantitated on Odyssey LICOR
667 imaging system. Plotted is the AR signal normalized to total CHK2 and compared to
668 untreated cells, n=3. Error bars, SEM. Statistical differences were tested for using ANOVA
669 with Sidak's multiple comparisons test. (B) Expression of CHK2 variants with reduced
670 kinase activity inhibits the radiation-induced increase in AR – CHK2 interactions. LNCaP

671 cells were transfected with HA-wtAR, HA-S81A, or HA-S308 in combination with FLAG-
672 wtCHK2 for 48hrs using TransIT-2020 (Mirus). Cells were irradiated with 6Gy, and FLAG
673 was immunoprecipitated using a magnetic bead system one hour after IR. Representative
674 blots are shown. Plotted is the HA-AR signal normalized to total FLAG-CHK2 and
675 compared to untreated cells. Error bars, SEM. Blots were quantitated on Odyssey LICOR
676 imaging system. Statistical differences were tested for using ANOVA with Sidak's multiple
677 comparisons test.
678
679 **Figure 3. Wild-type CHK2 negatively regulates prostate cancer cell growth.** (A)
680 LNCaP, (B) C4-2, and (C) Rv-1 cells were transduced with lentiviral particles expressing
681 vector, shCHK2-exon 12, or shCHK2-3'UTR in combination with wtCHK2, K373E, or
682 T387N in the presence or absence of 0.05nM R1881. CyQuant assay was performed 7
683 days after transduction. Cell growth was compared with untreated vector control and the
684 values were averaged across biological replicates. Error bars, SEM, n=3. Statistical
685 analysis was performed using ANOVA and Tukey test, * = $p<0.01$. Representative blots
686 of CHK2 expression are shown with ERK as a loading control.
687
688 **Figure 4. CHK2 knockdown increases the transcription of DDR genes in the**
689 **presence and absence of radiation.** Transcript levels of DDR genes in LNCaP cells
690 transduced with CHK2 shRNAs and pLKO vector control and grown in CSS
691 supplemented with 1nM DHT were measured by qPCR. 48hrs following transduction,
692 cells were exposed to 2Gy ionizing radiation and RNA was isolated 6 hours later.
693 Transcript levels were normalized to the housekeeping gene, PSMB6, and compared to

694 pLKO. Values were averaged across biological replicates +/- standard error of the mean,
695 n=3. Shown are the histograms for (A) DNAPKc and (B) Rad54B in LNCaP cells.
696 Statistical analysis was performed using one-way ANOVA and Tukey's test. * = $p<0.02$.
697
698 **Figure 5. CHK2-depleted cells show increased survival and reduced DNA damage**
699 **following radiation.** (A) Knockdown of CHK2 desensitizes cells to IR. LNCaP cells were
700 transduced with lentiviral particles expressing pLKO or CHK2 shRNAs for 48hrs, treated
701 with 0-6Gy IR, and seeded at the appropriate cell number for colony survival assays.
702 Results were normalized to untreated pLKO control and fitted to a standard linear
703 quadratic model. Error bars, SEM. Statistical analysis was performed using the Student's
704 t-test, n=4-8, $p<0.01$. (B) LNCaP cells were seeded in whole media for 48 hours, irradiated
705 at the indicated doses at the specified times and processed for comet assays. Shown is
706 the %DNA in the comet tail, comet tail length, and tail moment (% DNA x tail length), n=3
707 (209-592 cells measured per condition), 5-95% confidence intervals. Right most plots are
708 of pLKO and CHK2 KD at 24hrs to illustrate the statistical difference marked on the
709 graphs. Statistical differences were tested for using Kruskal-Wallis test followed by
710 Dunn's multiple comparisons test.
711
712 **Figure 6. CHK2-depleted cells show altered γH2AX foci kinetics.** (A) Representative
713 images of γH2AX, CHK2, and AR immunostaining quantified in (B and C). (B) Rv1 cells
714 were transduced with lentiviral particles expressing empty vector or CHK2 shRNAs on
715 fibronectin-coated coverslips in the appropriate growth media. Cells were irradiated with
716 6Gy after 48hrs. Coverslips were processed for IF at 0, 15min, 2, 4, and 24hrs following

717 IR. Plotted is the (B) γH2AX signal and (C) 53BP1 signal, which equals the mean grey
718 value intensity x number of foci per nucleus, n=3 (378-565 nuclei measured per
719 condition), 5-95% confidence intervals. Statistical differences were tested for using
720 Kruskal-Wallis test followed by Dunn's multiple comparisons test.
721
722 **Figure 7. Model of CHK2-AR.** We hypothesize the following model. In response to IR,
723 CHK2 activation antagonizes AR through direct binding and inhibition of transcription of
724 AR targets. CHK2 mutation or loss of expression that occurs in PCa leads to sustained
725 AR transcriptional activity, an increase in DDR gene transcripts, and survival in response
726 to DNA damage.
727

728 **Supplemental Figure 1. Far Western Blot schematic.** Purified proteins are separated
729 by SDS-PAGE (target proteins) and then transferred to a membrane. Proteins on the
730 membrane are renatured and then probed with purified proteins (probe), cross-linked, and
731 subsequently detected with antibodies.
732
733 **Supplemental Figure 2. AR S81 and S308 phosphorylation are not altered with**
734 **radiation.** LNCaP and C4-2 cells were seeded in serum-supplemented growth media for
735 48hrs, exposed to 6Gy IR, and AR was immunoprecipitated using a magnetic bead
736 system 1hr after radiation from 1mg cell extracts. Proteins were separated by 7.5% SDS-
737 PAGE, and blotted with AR, pAR S81, pAR S308, CHK2, and ERK1/2. Representative
738 blots are shown. Plotted is the pAR signal normalized to total AR and compared to
739 untreated cells, n=3, no statistical difference between the groups by ANOVA. Blots were
740 quantitated on Odyssey LICOR imaging system.
741
742 **Supplemental Figure 3. Automated quantitation of foci.** Confocal images are captured
743 on a Zeiss LSM 880 at 40x oil using Zeiss Zen digital imaging software and processed
744 into individual TIFF files for each fluorescence channel using ImageJ. An outline of nuclei
745 (mask) from DAPI channel is created and applied to all channels. Macro-enabled image
746 processing to measure multiple fluorescence parameters with background subtraction
747 using the following parameters: area, IntDen, RawIntDen, Min and Max, fluorescence,
748 background, foci count, CorDen, CorMean. γH2AX signal is the product of foci number
749 per nuclei and mean grey value (IntDen/area).
750

751 **Supplemental Figure 4. CHK2 Knockdown does not alter hormone induced γH2AX**
752 **foci.** LNCaP and Rv1 cells were transduced with lentiviral particles expressing empty
753 vector or CHK2 shRNA on fibronectin-coated coverslips in whole media for 48hrs. Media
754 was changed to CSS overnight and cells were treated with hormone for 6 hours. Plotted
755 is the number of γH2AX foci per cell. n=3 for LNCaP and n=2 for Rv1. At the same dose
756 of hormone there was no statistical difference between vector control and CHK2
757 knockdown by Kruskal-Wallis test followed by Dunn's multiple comparisons test.
758
759 **Supplemental Figure 5. Non-cropped images of Western blots shown in the**
760 **manuscript.**

A

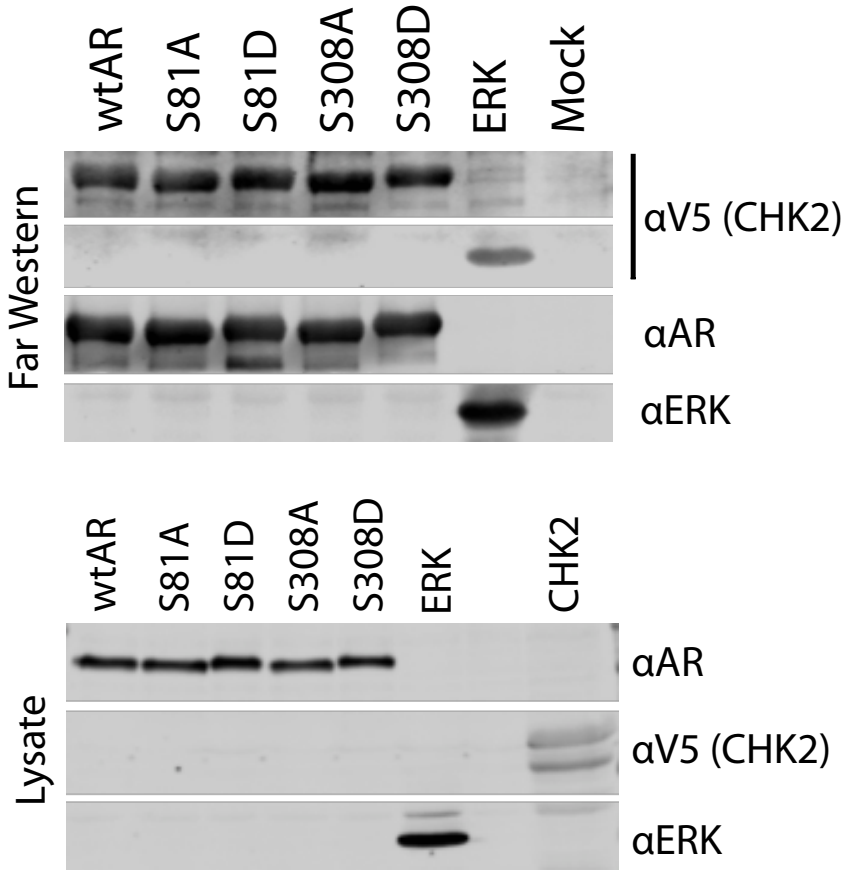
wtAR
S81A
S81D
S308A
S308D
ERK
Mock
Far Western
αV5 (CHK2)
αAR
αERK
wtAR
S81A
S81D
S308A
S308D
ERK
CHK2
Lysate
αAR
αV5 (CHK2)
αERK

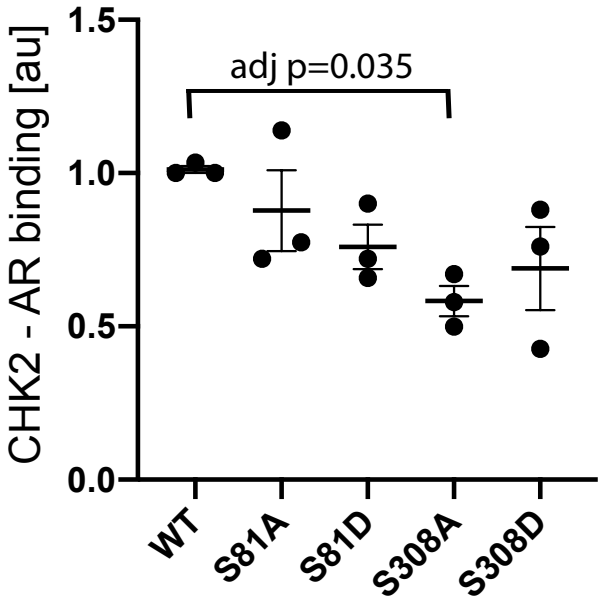
CHK2 - AR binding [au]
1.5
1.0
0.5
0.0
adj p=0.035
WT
S81A
S81D
S308A
S308D

B

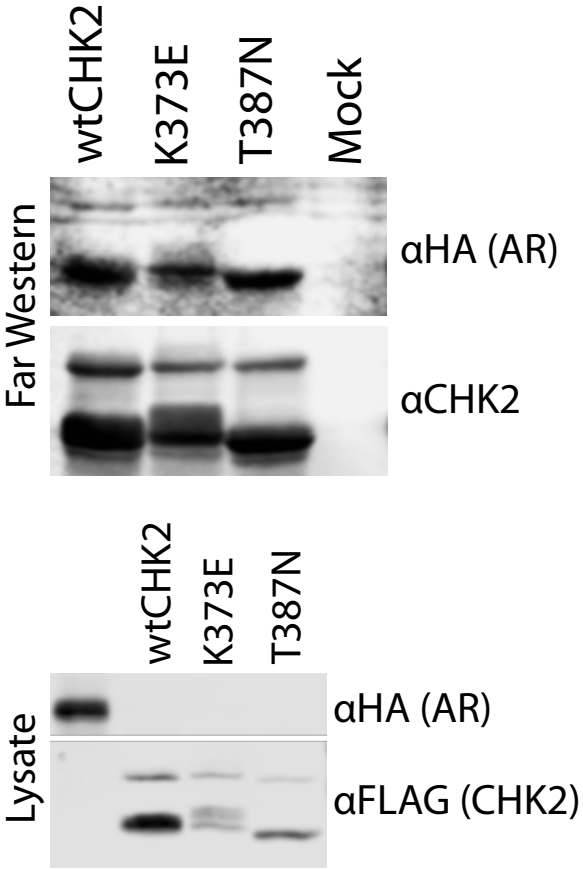
wtCHK2
K373E
T387N
Mock
Far Western
αHA (AR)
αCHK2
wtCHK2
K373E
T387N
Lysate
αHA (AR)
αFLAG (CHK2)

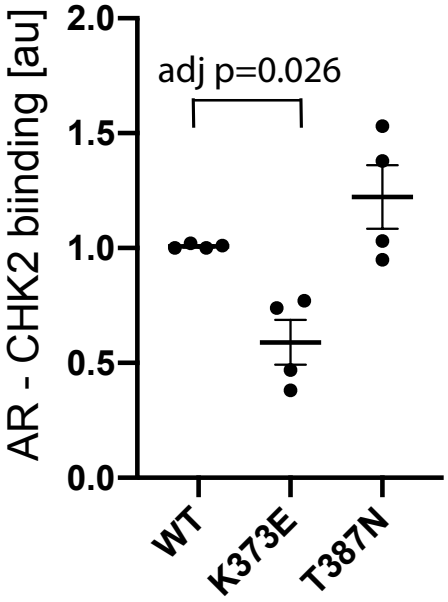
AR - CHK2 biinding [au]
2.0
1.5
1.0
0.5
0.0
adj p=0.026
WT
K373E
T387N

Figure 1

A

CHK2 co-IP

S308A S81A wtAR

- + - + - + IR (6gy)

αAR

αCHK2

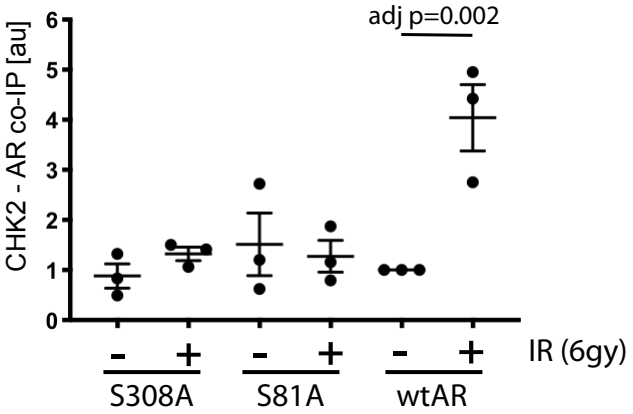

B

CHK2 co-IP

wtCHK2 K373E T387N

- + - + - + IR (6gy)

αHA

αCHK2

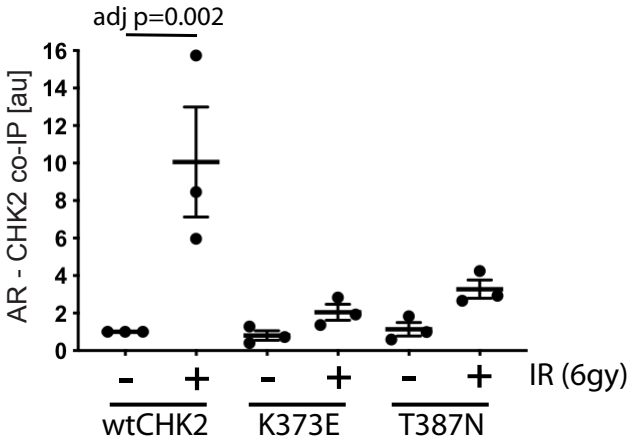

C

Lysate

wtAR S81A S308A

- + - + - + IR (6gy)

αAR

αCHK2

Lysate

wtCHK2 K373E T387N

- + - + - + IR (6gy)

αHA

αCHK2

αActin

Figure 2

A

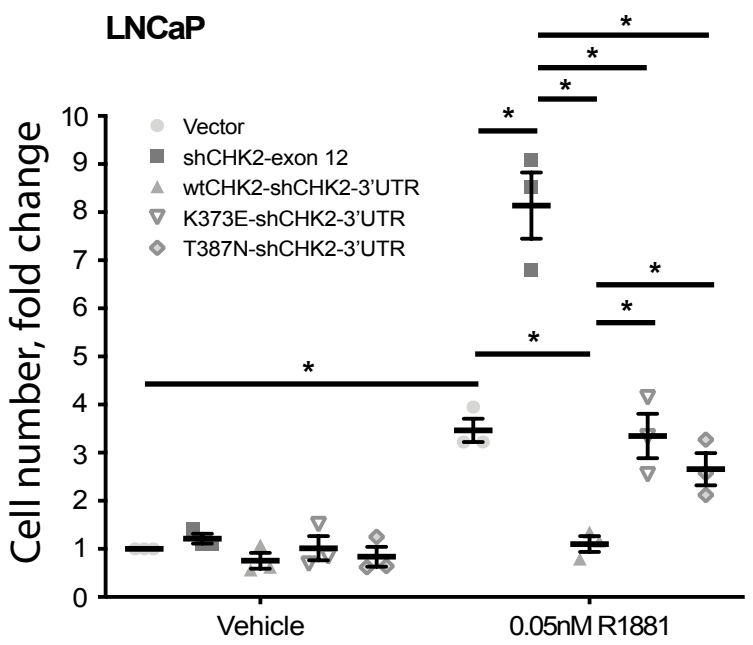

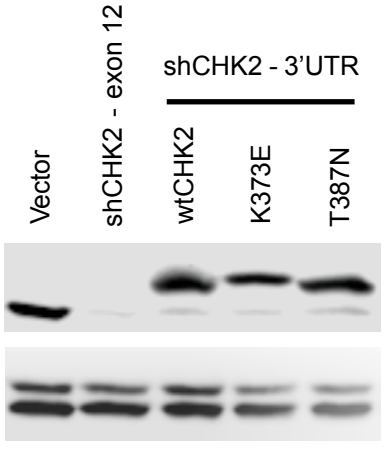

	Vector	shCHK2 - exon 12	wtCHK2	K373E	T387N	
CHK2ex:ERK1/2 Normalized to Vector	1.00		1.22 +/- 0.23	1.23 +/- 0.20	1.22 +/- 0.22	
CHK2ex:ERK1/2 Normalized to wtCHK2			1.00	1.03 +/- 0.07	1.01 +/- 0.03	

B

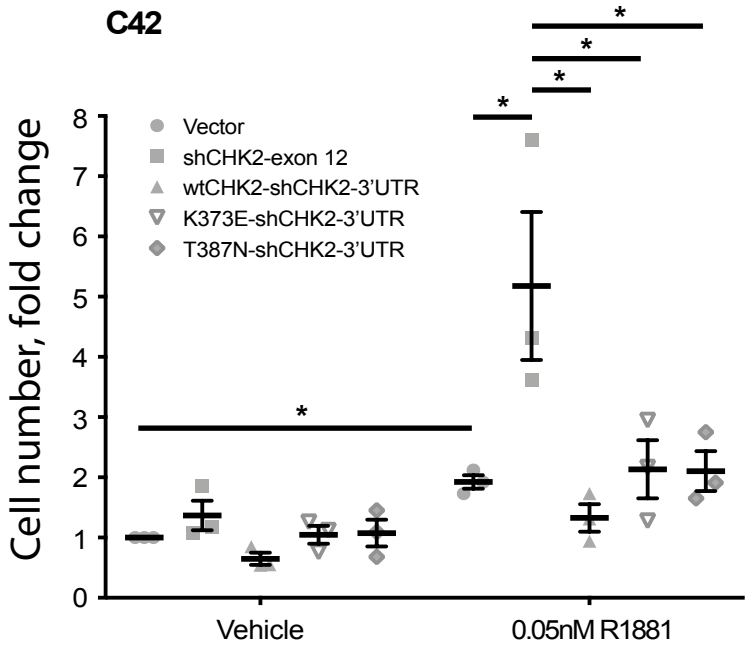

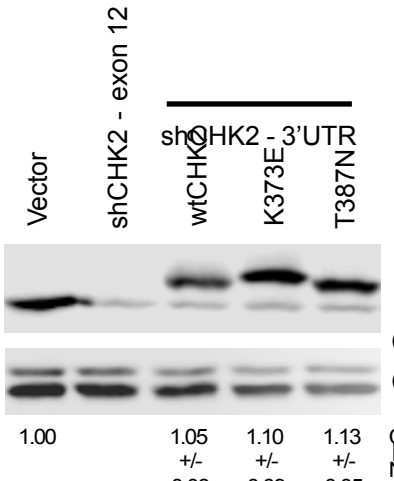

	Vector	shCHK2 - exon 12	wtCHK2	K373E	T387N	
CHK2ex:ERK1/2 Normalized to Vector	1.00		1.05 +/- 0.08	1.10 +/- 0.09	1.13 +/- 0.05	
CHK2:ERK1/2 Normalized to wtCHK2			1.00	1.06 +/- 0.01	1.09 +/- 0.11	

C

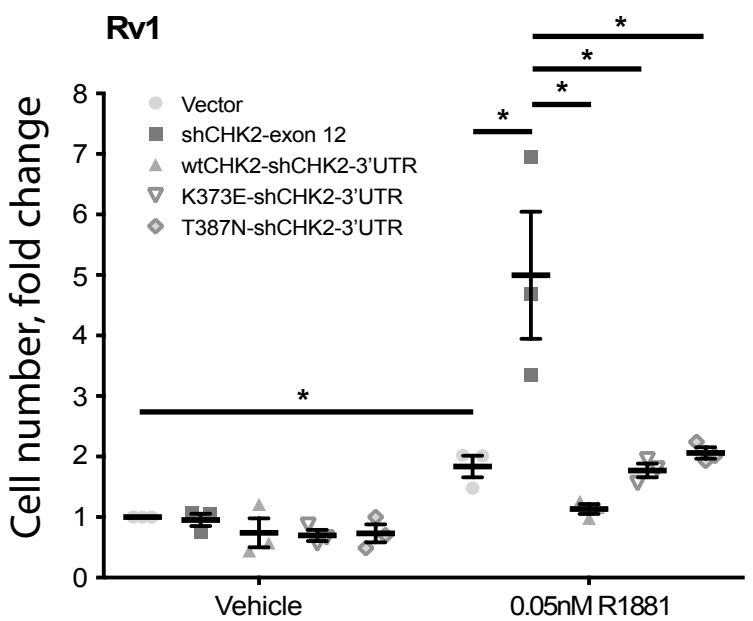

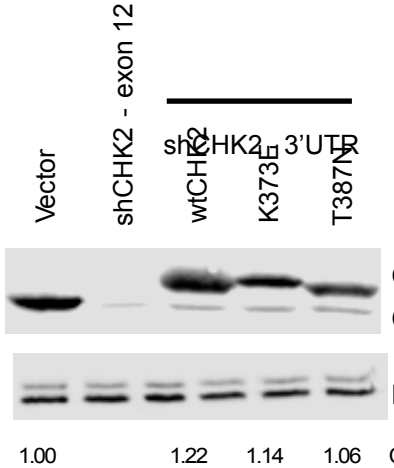

	Vector	shCHK2 - exon 12	wtCHK2	K373E	T387N	
CHK2ex:ERK1/2 Normalized to Vector	1.00		1.22 +/- 0.21	1.14 +/- 0.11	1.06 +/- 0.16	
CHK2ex:ERK1/2 Normalized to wtCHK2			1.00	0.97 +/- 0.10	0.88 +/- 0.05	

Figure 3

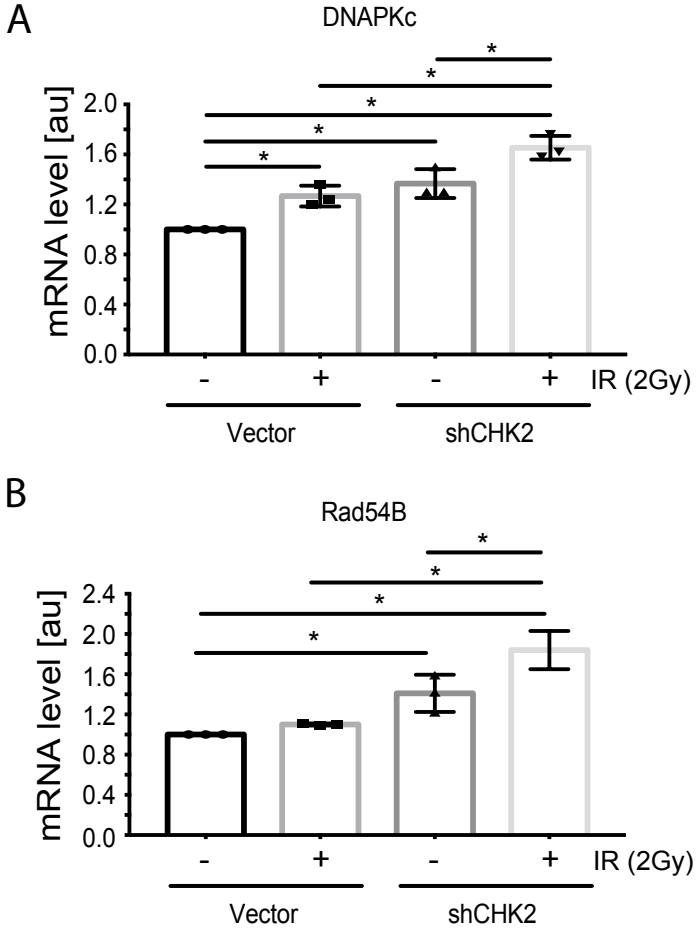
A
DNAPKc
mRNA level [au]
2.0
1.6
1.2
0.8
0.4
0.0
*
*
*
*
*
-
+
-
+
IR (2Gy)
Vector
shCHK2
B
Rad54B
mRNA level [au]
2.4
2.0
1.6
1.2
0.8
0.4
0.0
*
*
*
*
-
+
-
+
IR (2Gy)
Vector
shCHK2

Figure 4

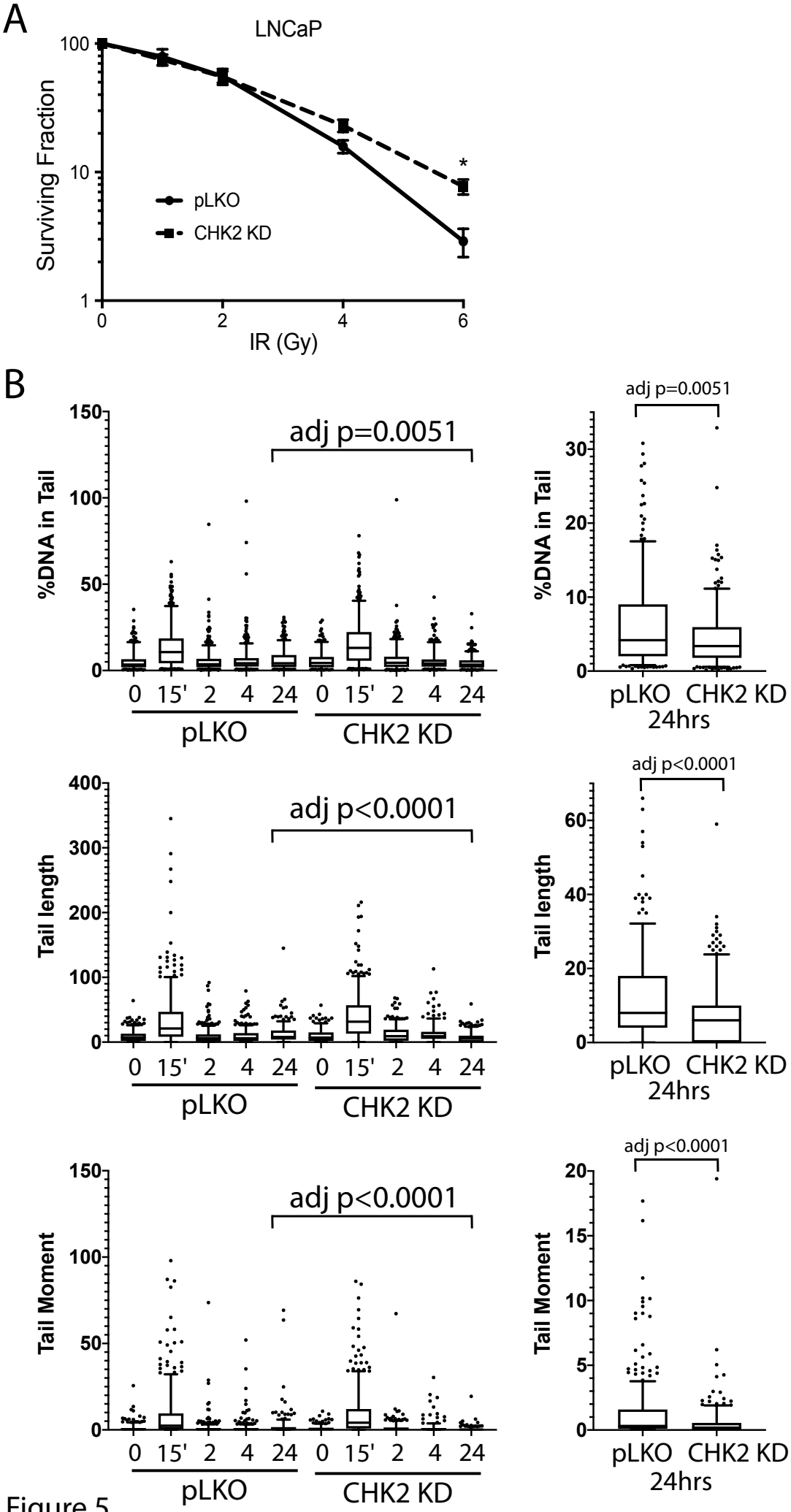
A
LNCaP
Surviving Fraction
100
10
1
0
2
4
6
IR (Gy)
pLKO
CHK2 KD
*
B
%DNA in Tail
adj p=0.0051
150
100
50
0
0 15' 2 4 24 0 15' 2 4 24
pLKO
CHK2 KD
adj p=0.0051
30
20
10
0
pLKO CHK2 KD
24hrs
Tail length
adj p<0.0001
400
300
200
100
0
0 15' 2 4 24 0 15' 2 4 24
pLKO
CHK2 KD
adj p<0.0001
60
40
20
0
pLKO CHK2 KD
24hrs
Tail Moment
adj p<0.0001
150
100
50
0
0 15' 2 4 24 0 15' 2 4 24
pLKO
CHK2 KD
adj p<0.0001
20
15
10
5
0
pLKO CHK2 KD
24hrs

Figure 5

A

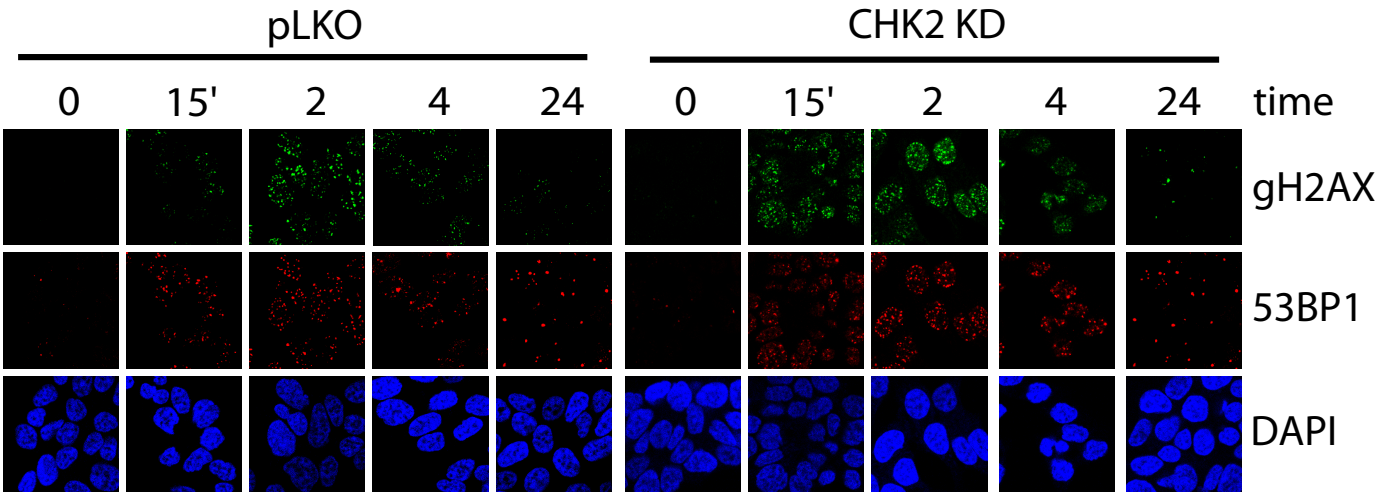
pLKO
CHK2 KD
0
15'
2
4
24
0
15'
2
4
24
time
gH2AX
53BP1
DAPI

B

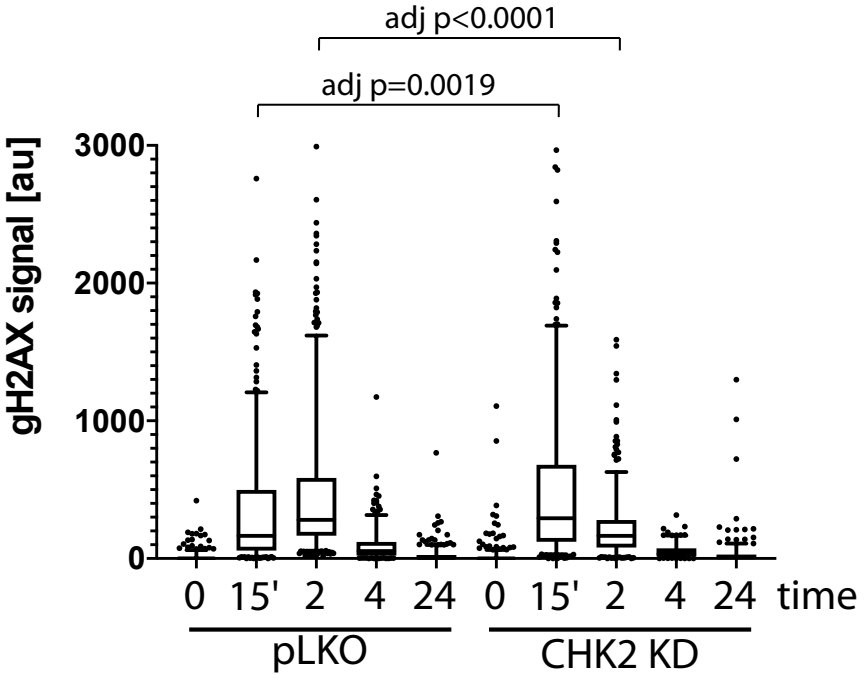
adj p<0.0001
adj p=0.0019
gH2AX signal [au]
3000
2000
1000
0
0
15'
2
4
24
0
15'
2
4
24
time
pLKO
CHK2 KD

C

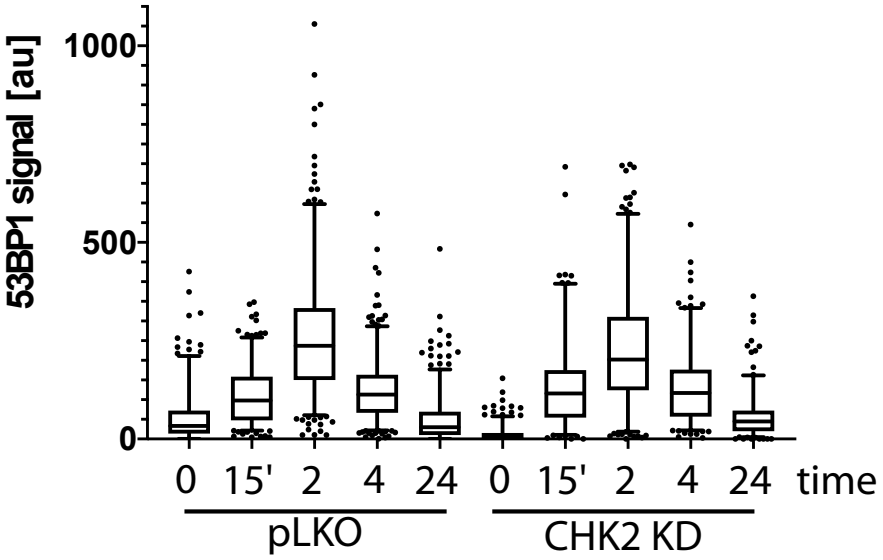
53BP1 signal [au]
1000
500
0
0
15'
2
4
24
0
15'
2
4
24
time
pLKO
CHK2 KD

Figure 6

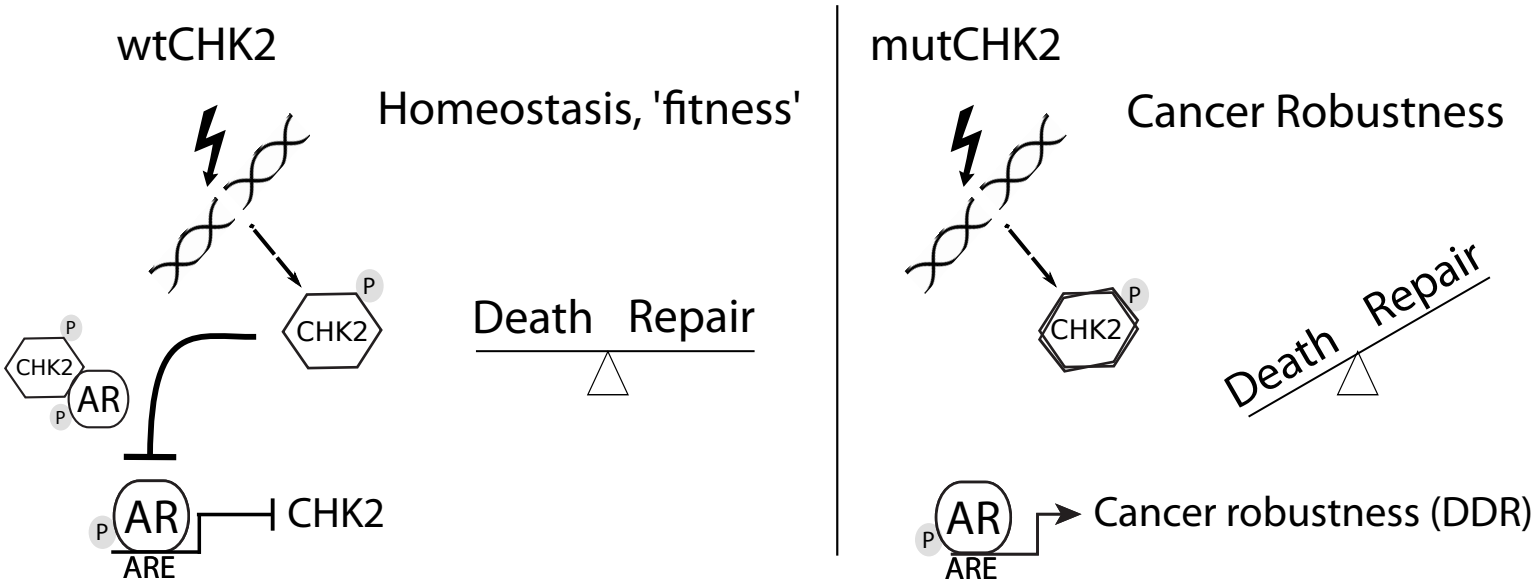
wtCHK2
Homeostasis, 'fitness'
P
CHK2
P
CHK2
AR
P
Death
Repair
P
AR
CHK2
ARE
mutCHK2
Cancer Robustness
P
CHK2
Death
Repair
P
AR
Cancer robustness (DDR)
ARE

Figure 7---

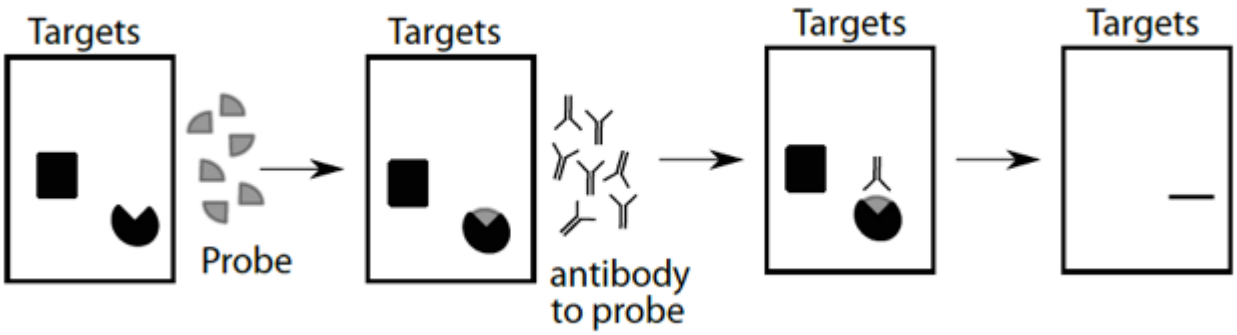

Supplemental Figure 1

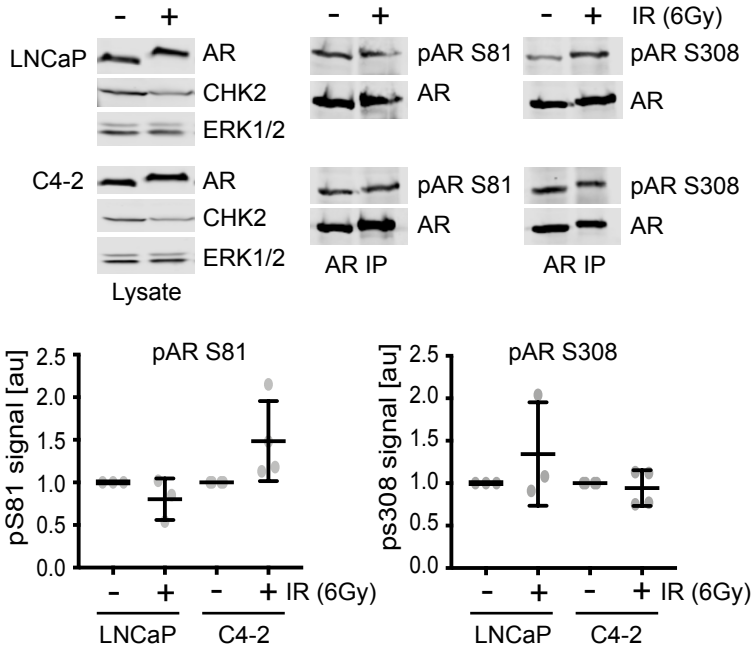

Supplemental Figure 2

1) Create a mask from DAPI channel

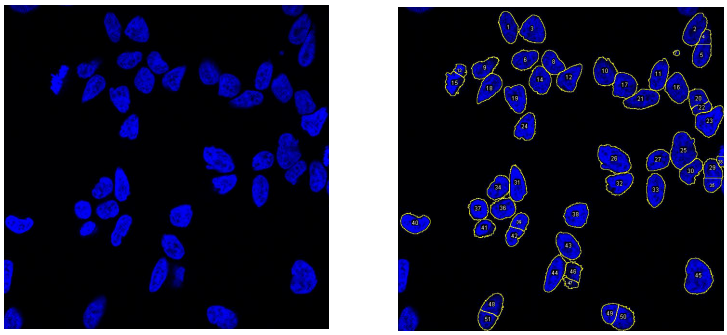

2) Apply DAPI mask onto the gH2AX channel

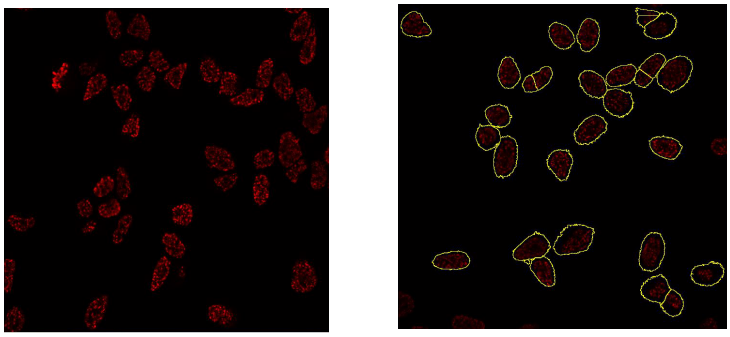

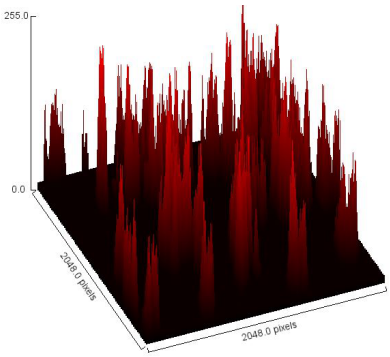

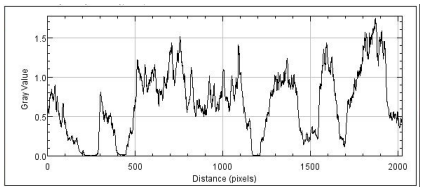

3) Background subtraction

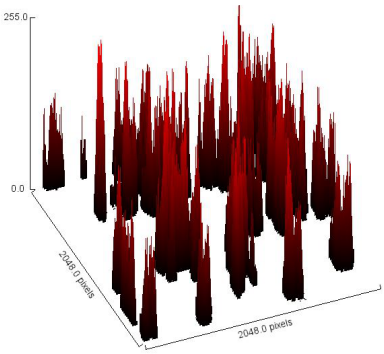

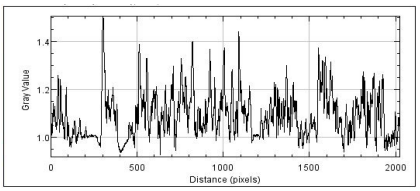

4) Maxima points (foci)

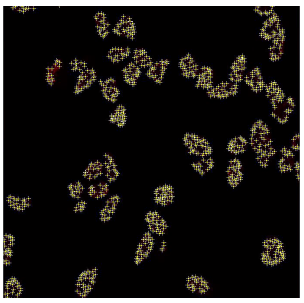

Example of output

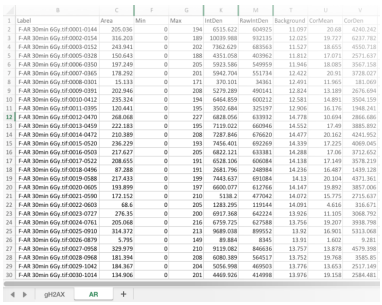

	B	C	F	G	K	M	T	U	V
1	Label	Area	Min	Max	IntDen	RawIntDen	Background	CorMean	CorDen
2	F-AR 30min 6Gy.tif:0001-0144	205.036	0	194	6515.622	604925	11.097	20.68	4240.242
3	F-AR 30min 6Gy.tif:0002-0154	316.203	0	189	10039.988	932135	12.025	19.727	6237.782
4	F-AR 30min 6Gy.tif:0003-0152	243.941	0	202	7362.629	683563	11.527	18.655	4550.718
5	F-AR 30min 6Gy.tif:0005-0328	150.643	0	188	4351.058	403962	11.812	17.071	2571.637
6	F-AR 30min 6Gy.tif:0006-0350	197.249	0	205	5923.586	549959	11.946	18.085	3567.158
7	F-AR 30min 6Gy.tif:0007-0365	178.292	0	201	5942.704	551734	12.422	20.91	3728.027
8	F-AR 30min 6Gy.tif:0008-0301	15.133	0	171	370.101	34361	12.491	11.965	181.069
9	F-AR 30min 6Gy.tif:0009-0391	202.946	0	208	5279.289	490141	12.824	13.189	2676.694
10	F-AR 30min 6Gy.tif:0010-0412	235.324	0	194	6464.859	600212	12.581	14.891	3504.159
11	F-AR 30min 6Gy.tif:0011-0395	120.441	0	195	3502.684	325197	12.906	16.176	1948.241
12	F-AR 30min 6Gy.tif:0012-0470	268.068	0	227	6828.056	633932	14.778	10.694	2866.686
13	F-AR 30min 6Gy.tif:0013-0459	222.183	0	195	7119.022	660946	14.552	17.49	3885.892
14	F-AR 30min 6Gy.tif:0014-0472	210.389	0	208	7287.846	676620	14.477	20.162	4241.952
15	F-AR 30min 6Gy.tif:0015-0520	236.229	0	193	7456.401	692269	14.339	17.225	4069.045
16	F-AR 30min 6Gy.tif:0016-0503	217.627	0	205	6822.121	633381	14.288	17.06	3712.652
17	F-AR 30min 6Gy.tif:0017-0522	208.655	0	191	6528.106	606084	14.138	17.149	3578.219
18	F-AR 30min 6Gy.tif:0018-0496	87.288	0	191	2681.796	248984	14.236	16.487	1439.128
19	F-AR 30min 6Gy.tif:0019-0588	217.433	0	199	7443.637	691084	14.13	20.104	4371.361
20	F-AR 30min 6Gy.tif:0020-0605	193.899	0	197	6600.077	612766	14.147	19.892	3857.006
21	F-AR 30min 6Gy.tif:0021-0590	172.152	0	210	5138.2	477042	14.072	15.775	2715.637
22	F-AR 30min 6Gy.tif:0022-0603	68.6	0	205	1283.295	119144	14.091	4.616	316.671
23	F-AR 30min 6Gy.tif:0023-0727	276.35	0	200	6917.368	642224	13.926	11.105	3068.792
24	F-AR 30min 6Gy.tif:0024-0761	205.068	0	216	6758.725	627588	13.756	19.207	3938.798
25	F-AR 30min 6Gy.tif:0025-0910	314.372	0	213	9689.038	899552	13.92	16.901	5313.068
26	F-AR 30min 6Gy.tif:0026-0879	5.795	0	149	89.884	8345	13.91	1.602	9.281
27	F-AR 30min 6Gy.tif:0027-0958	329.979	0	210	9119.082	846636	13.757	13.878	4579.398
28	F-AR 30min 6Gy.tif:0028-0968	181.394	0	208	6080.389	564517	13.752	19.768	3585.85
29	F-AR 30min 6Gy.tif:0029-1042	184.367	0	204	5056.998	469503	13.776	13.653	2517.149
30	F-AR 30min 6Gy.tif:0030-1014	134.906	0	201	4469.926	414998	13.976	19.158	2584.481

gH2AX AR

Supplemental Figure 3

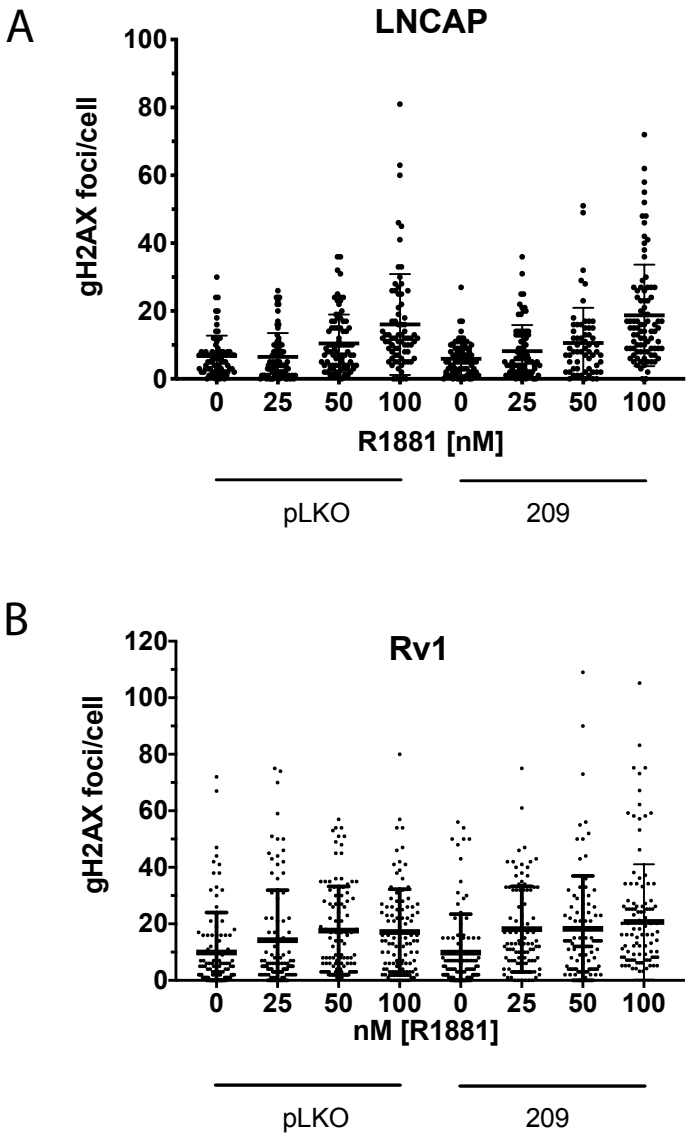

Supplemental Figure 4

Figure 1

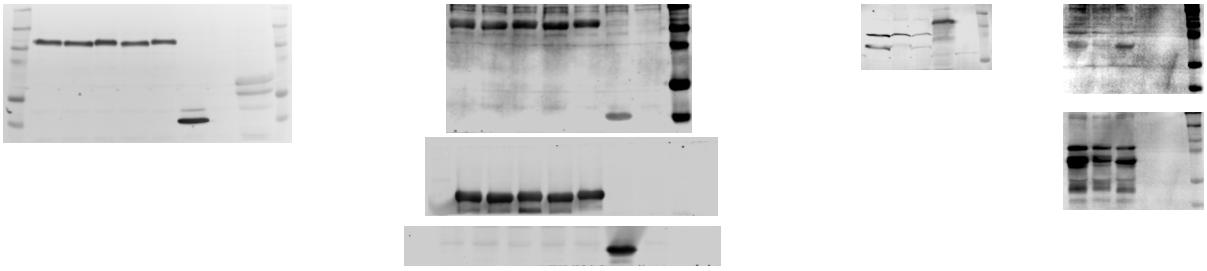

Figure 2

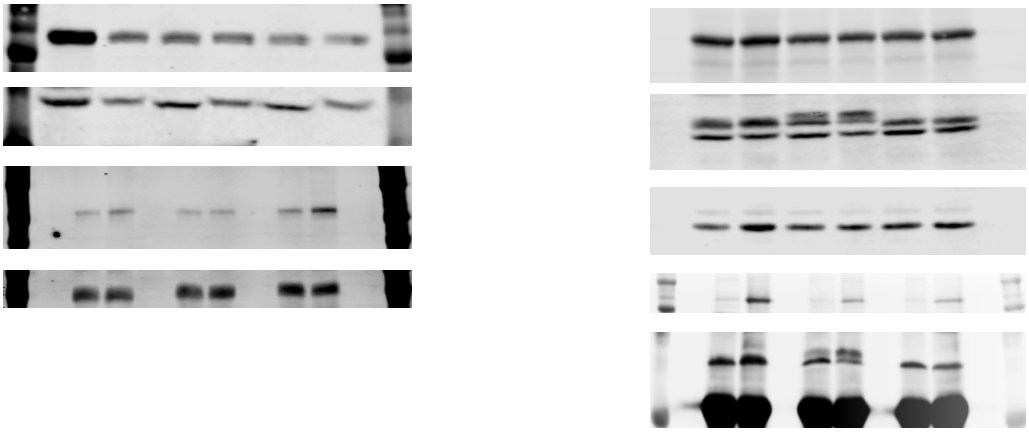

Figure 3

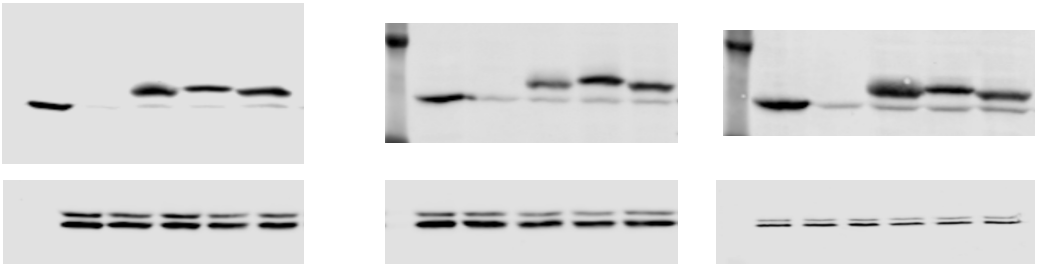

Supplemental Figure 5